Supporting Information

Alkylamido Lutetium Complexes as Prospective Lutetium Imido Precursors: Synthesis, Characterization and Ligand Design

Jackson P. Knott, Shou-Jen Hsiang, and Paul G. Hayes*

Department of Chemistry & Biochemistry, University of Lethbridge, Lethbridge, Alberta T1K 3M4 Canada

p.hayes@uleth.ca

Table of Contents

I. NMR Spectra

$L^{iPr}Sc(CH_2SiMe_3)_2$ (**5**):

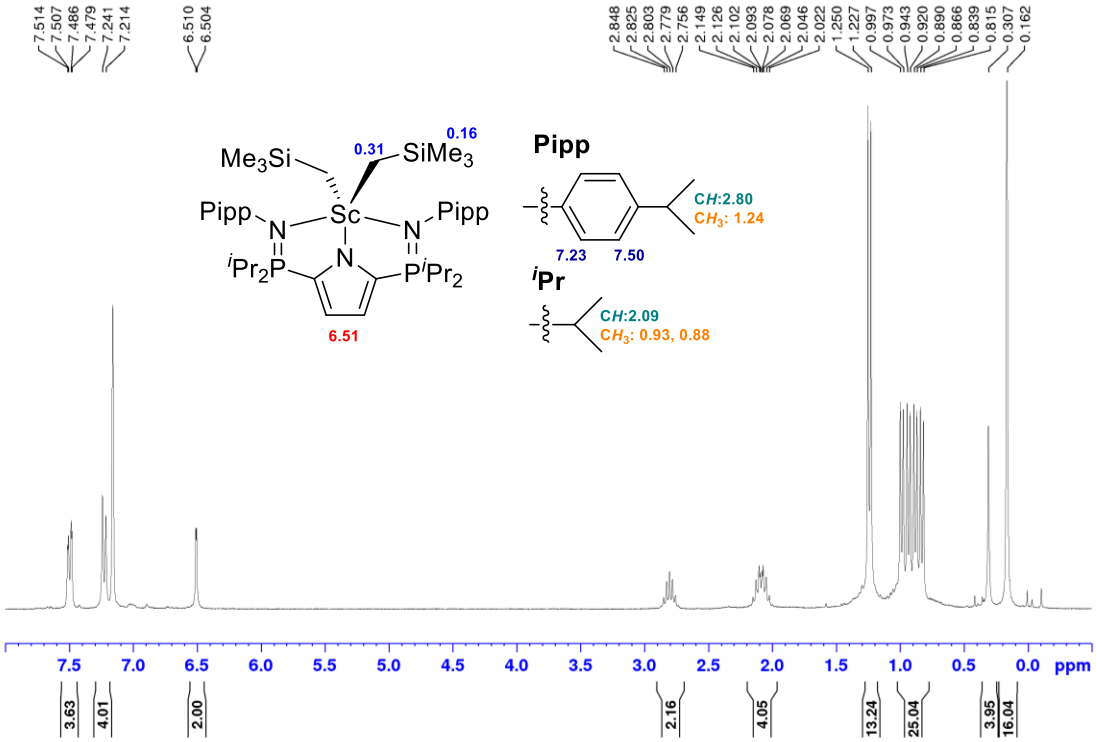

Figure S1. ^{1}H NMR Spectrum of $L^{iPr}Sc(CH_2SiMe_3)_2$ in benzene-d_6 at ambient temperature.

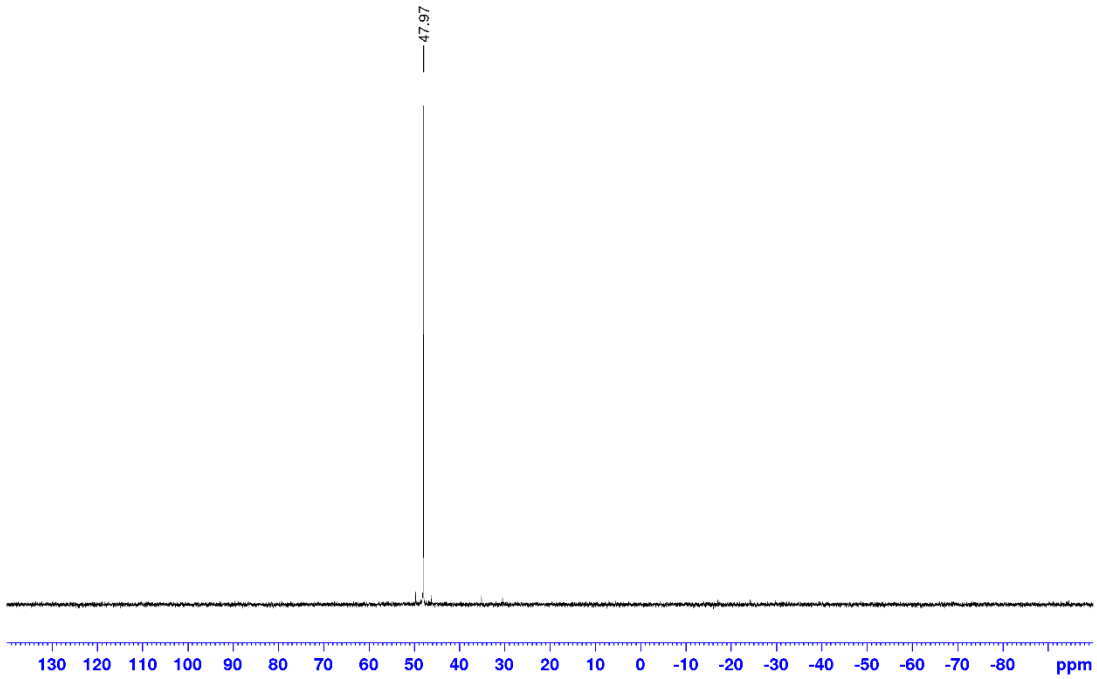

Figure S2. $^{31}P\{^1H\}$ NMR Spectrum of $L^{iPr}Sc(CH_2SiMe_3)_2$ in benzene-d_6 at ambient temperature.

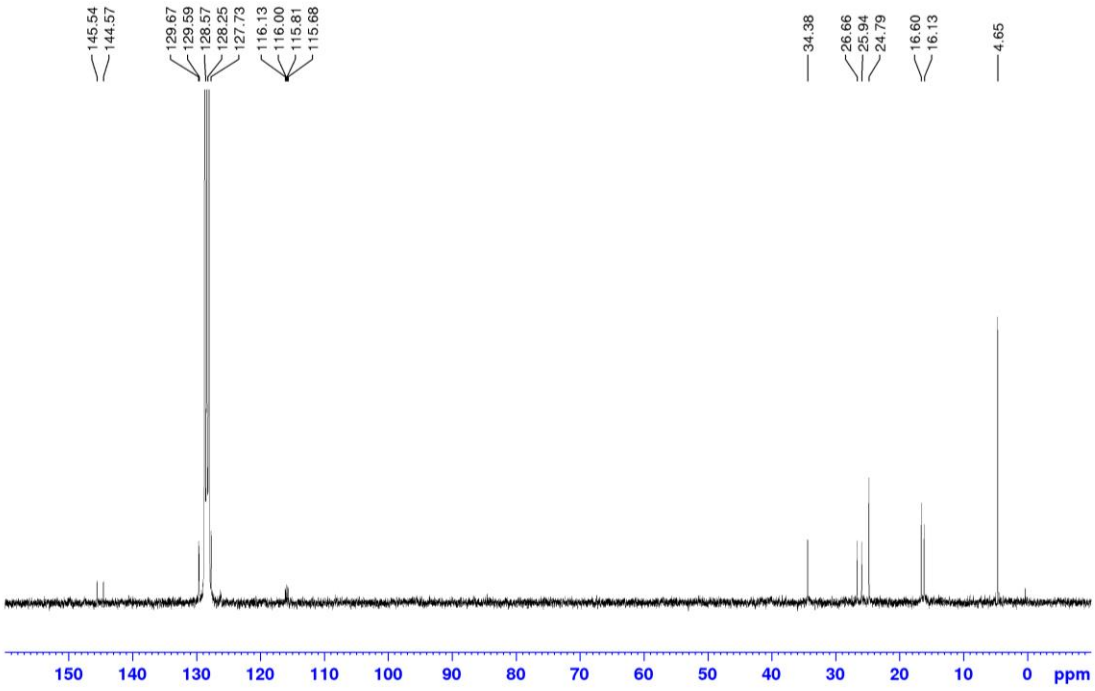

Figure S3. $^{13}C\{^{1}H\}$ NMR Spectrum of $L^{iPr}Sc(CH_2SiMe_3)_2$ in benzene-d_6 at ambient temperature.

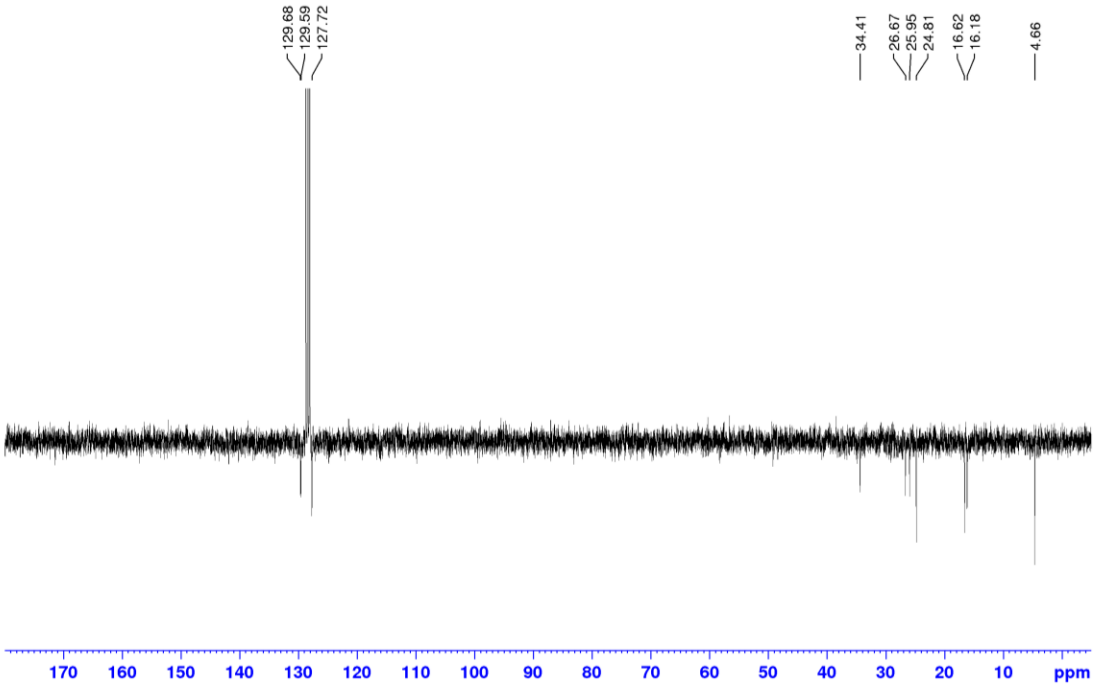

Figure S4. APT NMR Spectrum of $L^{iPr}Sc(CH_2SiMe_3)_2$ in benzene-d_6 at ambient temperature.

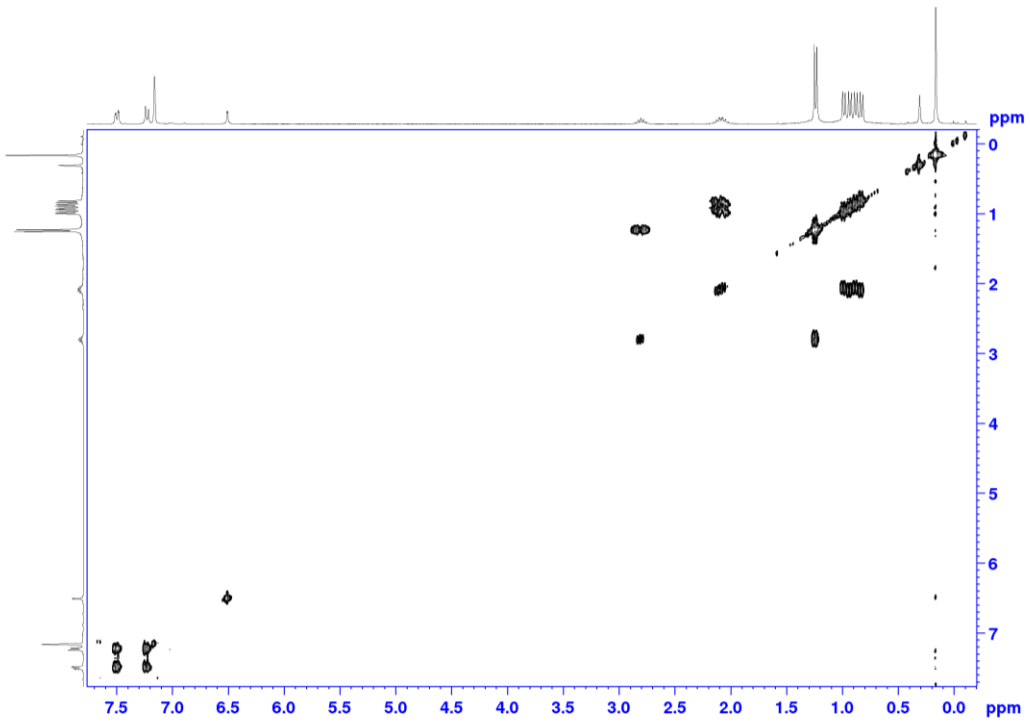

Figure S5. ^{1}H–^{1}H COSY NMR Spectrum of $L^{iPr}Sc(CH_2SiMe_3)_2$ in benzene-d_6 at ambient temperature.

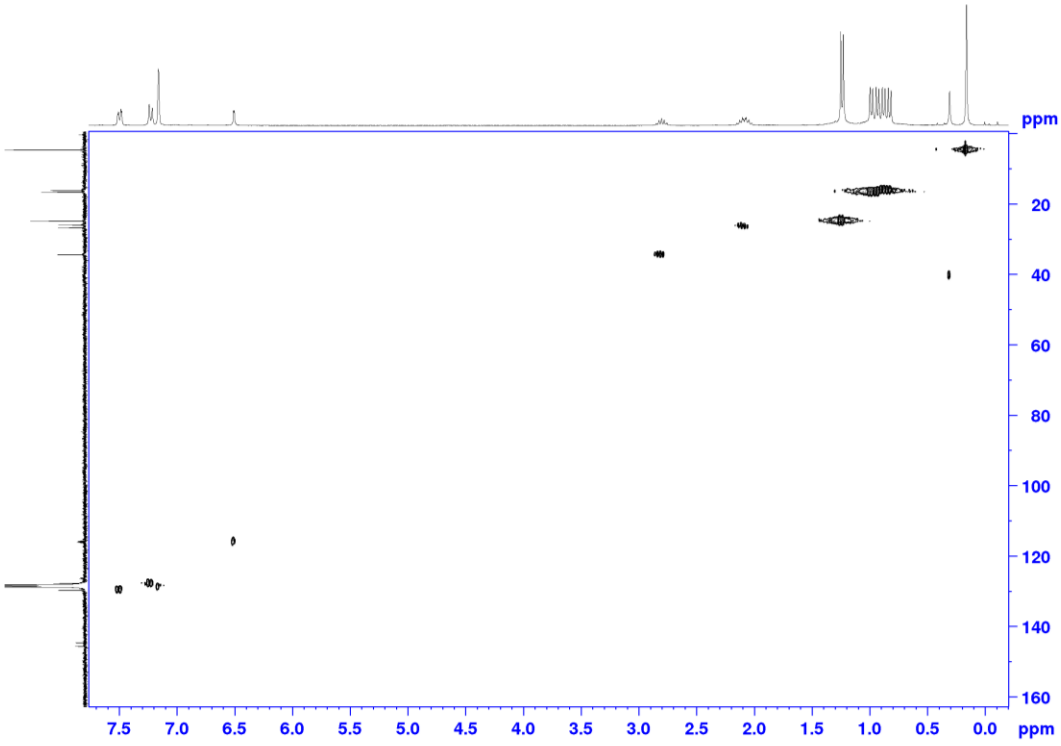

Figure S6. ^{1}H–^{13}C HSQC NMR Spectrum of $L^{iPr}Sc(CH_2SiMe_3)_2$ in benzene-d_6 at ambient temperature.

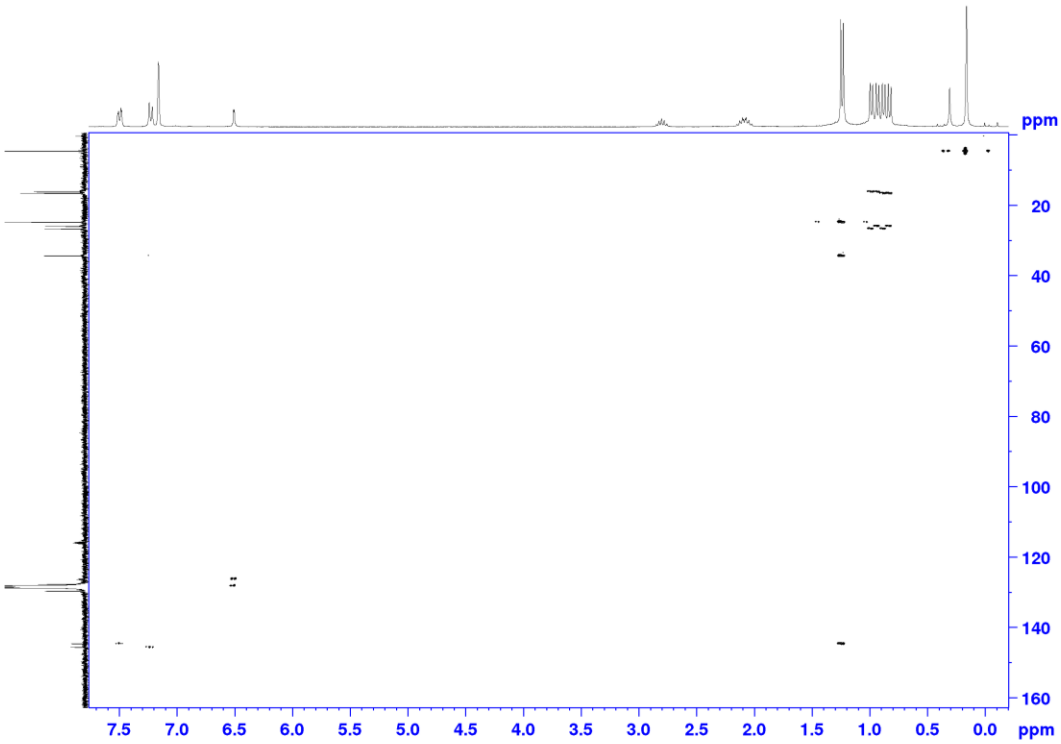

Figure S7. ^{1}H–^{13}C HMBC NMR Spectrum of $L^{iPr}Sc(CH_2SiMe_3)_2$ in benzene-d_6 at ambient temperature.

$L^{iPr}Lu(CH_2SiMe_3)_2$ (**6**):

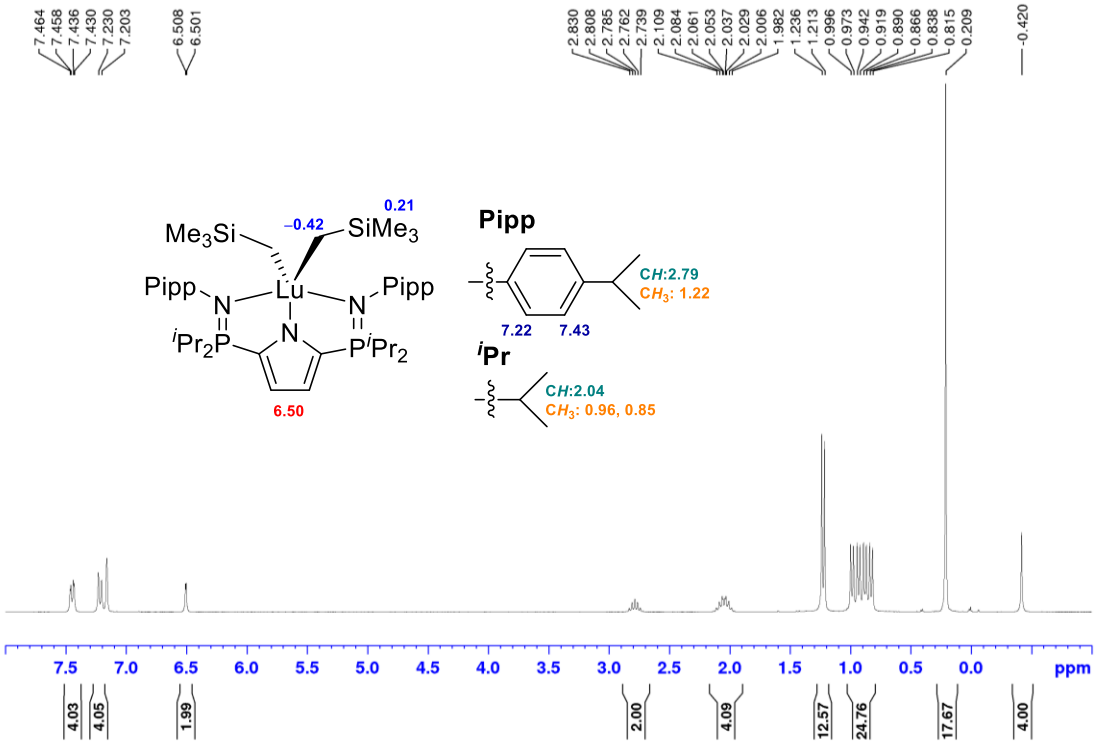

Figure S8. ^{1}H NMR Spectrum of $L^{iPr}Lu(CH_2SiMe_3)_2$ in benzene-d_6 at ambient temperature.

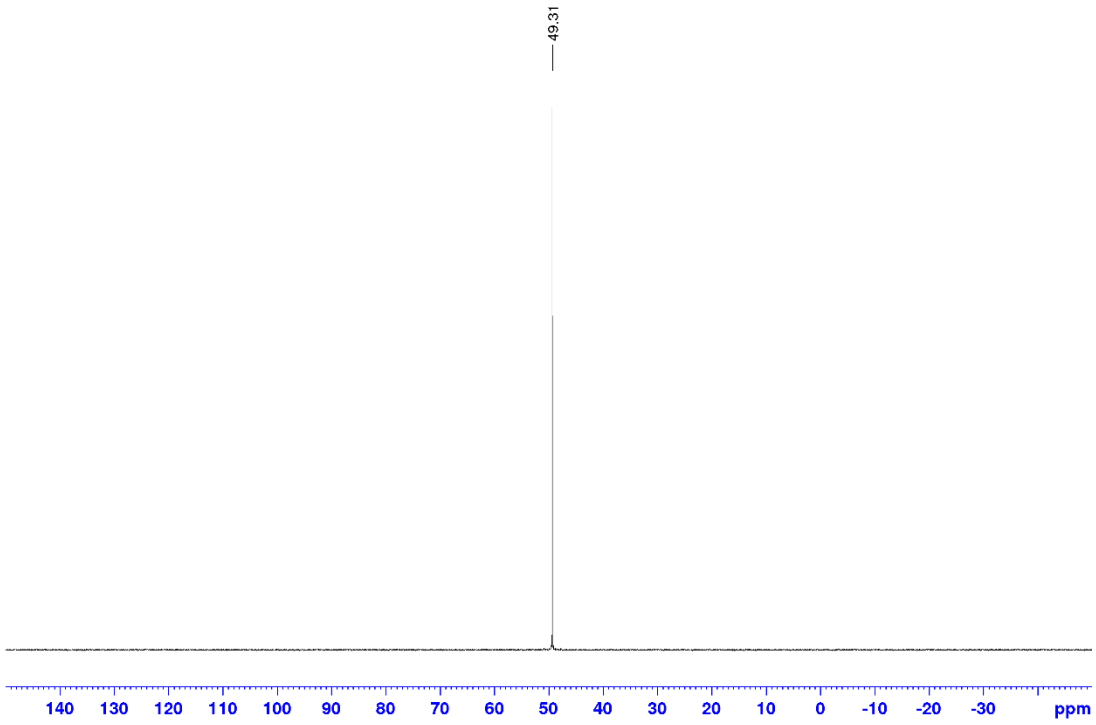

Figure S9. $^{31}P\{^{1}H\}$ NMR Spectrum of $L^{iPr}Lu(CH_2SiMe_3)_2$ in benzene-d_6 at ambient temperature.

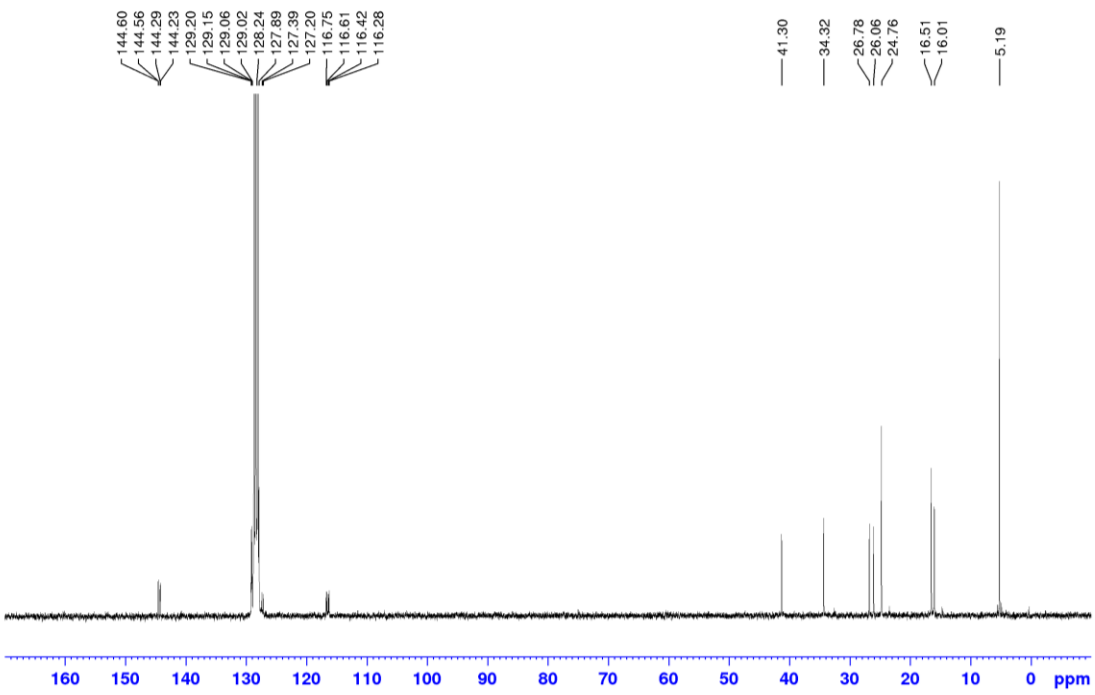

Figure S10. $^{13}C\{^{1}H\}$ NMR Spectrum of $L^{iPr}Lu(CH_2SiMe_3)_2$ in benzene-d_6 at ambient temperature.

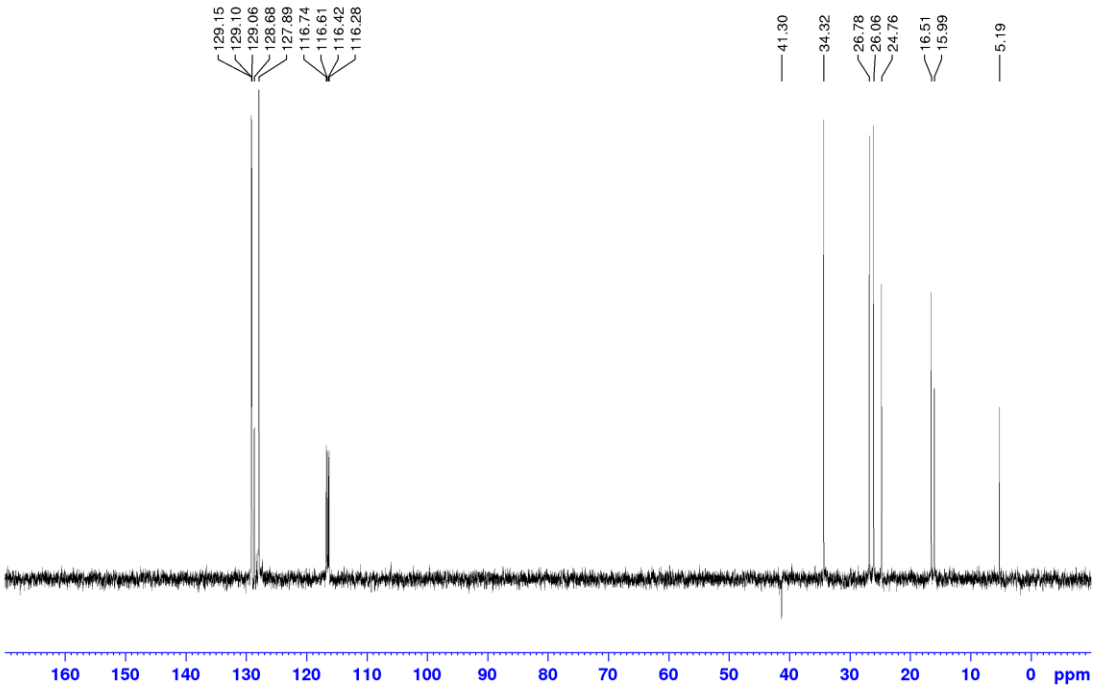

Figure S11. DEPT-135 NMR Spectrum of $L^{iPr}Lu(CH_2SiMe_3)_2$ in benzene-d_6 at ambient temperature.

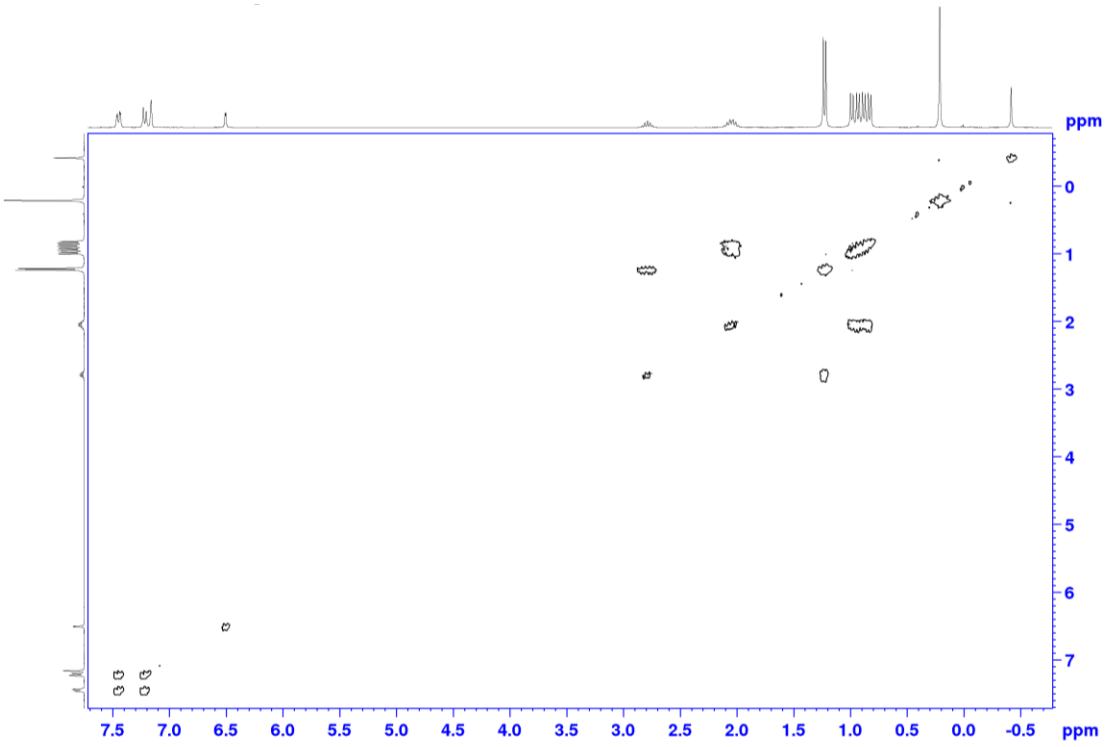

Figure S12. $^{1}H–^{1}H$ COSY NMR Spectrum of $L^{iPr}Lu(CH_2SiMe_3)_2$ in benzene-d_6 at ambient temperature.

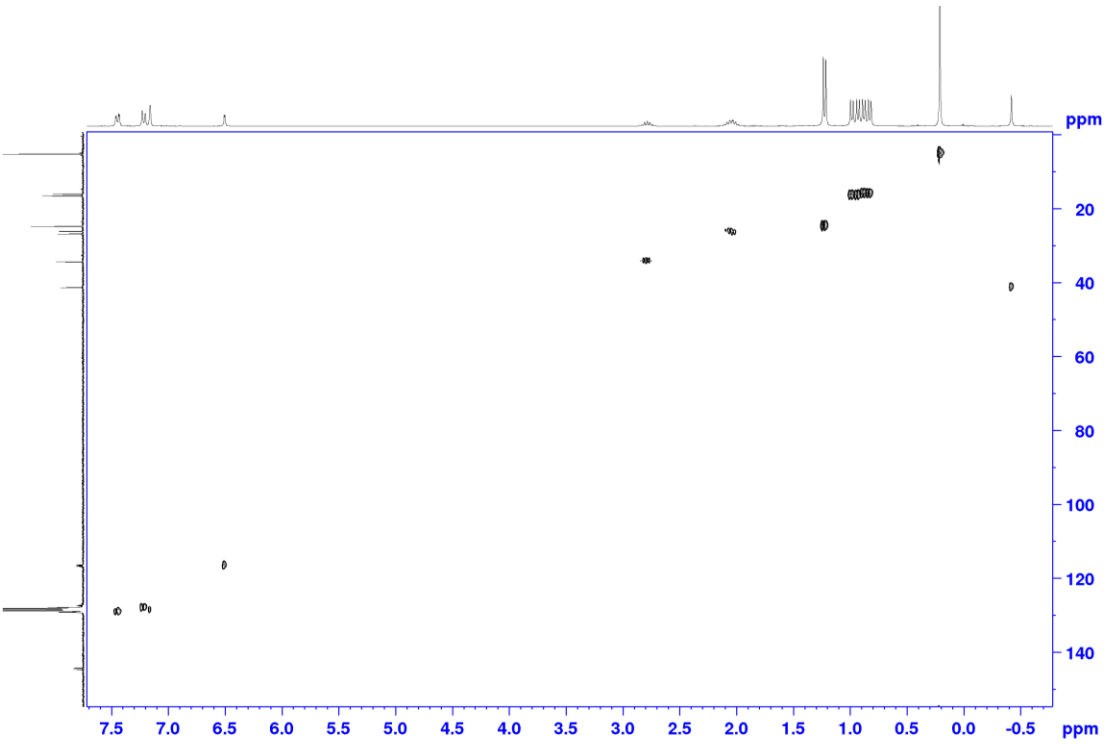

Figure S13. $^{1}H–^{13}C$ HSQC NMR Spectrum of $L^{iPr}Lu(CH_2SiMe_3)_2$ in benzene-d_6 at ambient temperature.

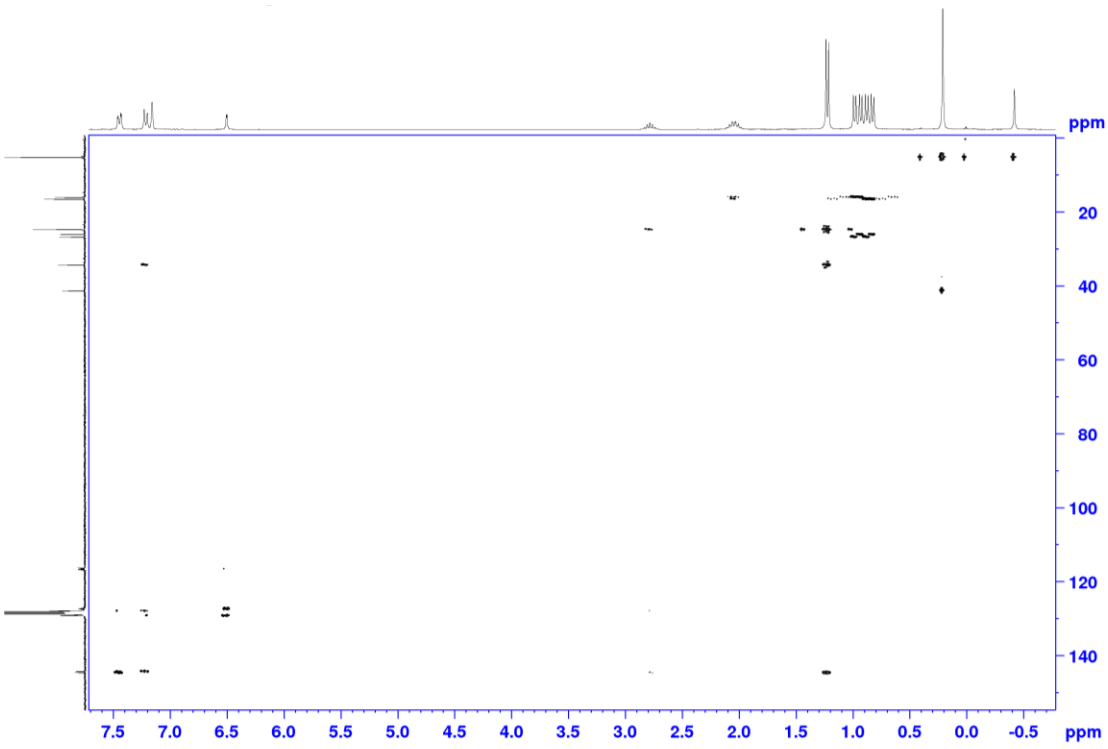

Figure S14. ^{1}H–^{13}C HMBC NMR Spectrum of $L^{iPr}Lu(CH_2SiMe_3)_2$ in benzene-d_6 at ambient temperature.

$L^{iPr}Lu(CH_2SiMe_3)(NHCPh_3)$ (**7_{CPh3}**):

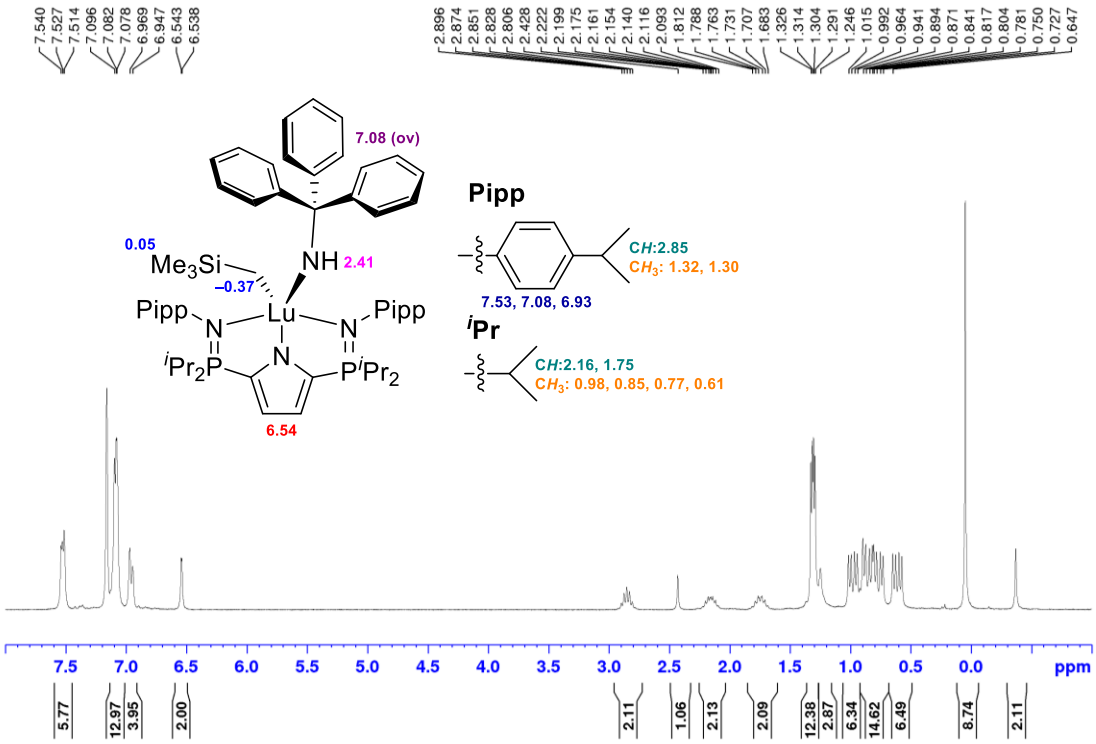

Figure S15. ^{1}H NMR Spectrum of $L^{iPr}Lu(CH_2SiMe_3)(NHCPh_3)$ in benzene-d_6 at ambient temperature.

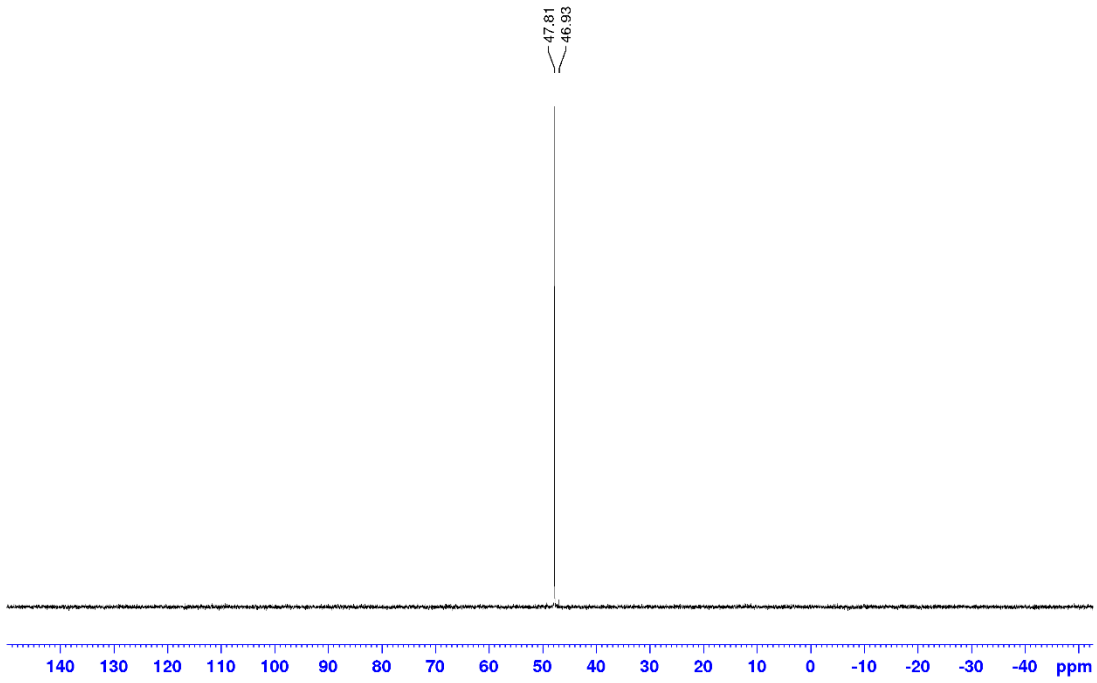

Figure S16. $^{31}P\{^{1}H\}$ NMR Spectrum of $L^{iPr}Lu(CH_2SiMe_3)(NHCPh_3)$ in benzene-d_6 at ambient temperature.

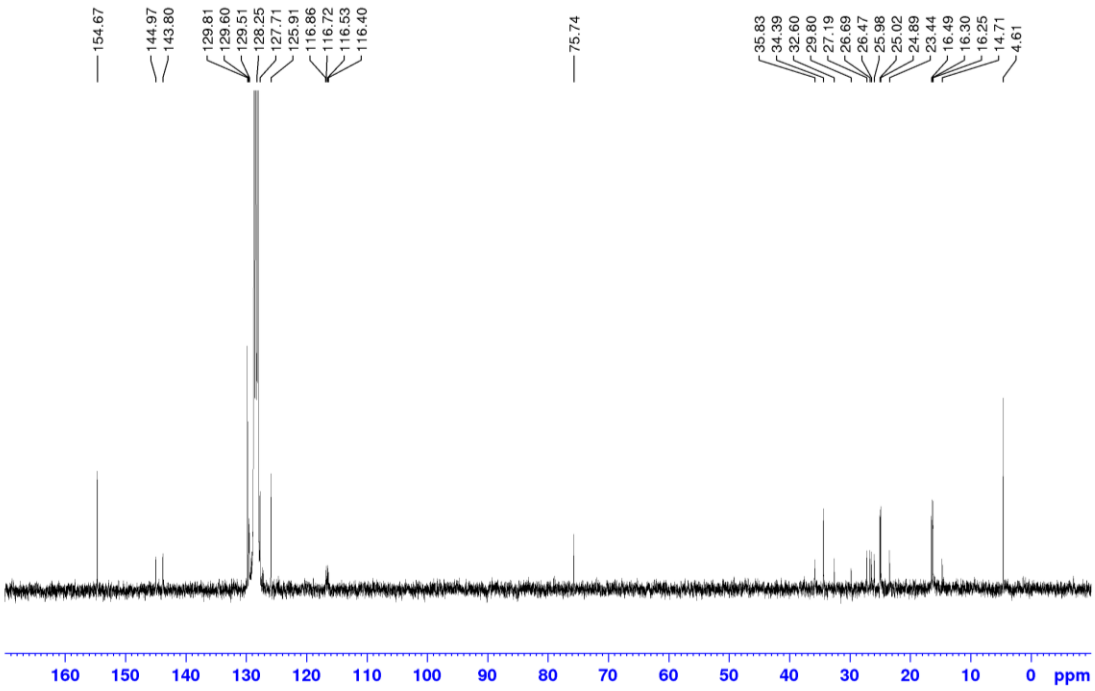

Figure S17. $^{13}C\{^{1}H\}$ NMR Spectrum of $L^{iPr}Lu(CH_2SiMe_3)(NHCPh_3)$ in benzene-d_6 at ambient temperature.

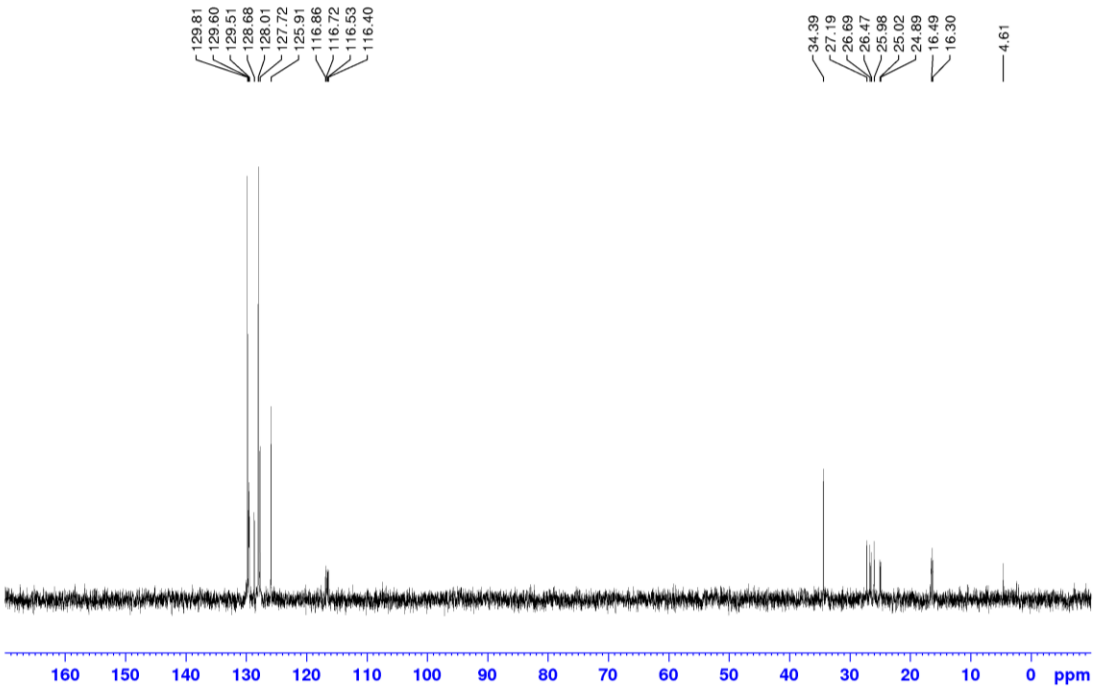

Figure S18. DEPT-135 NMR Spectrum of $L^{iPr}Lu(CH_2SiMe_3)(NHCPh_3)$ in benzene-d_6 at ambient temperature.

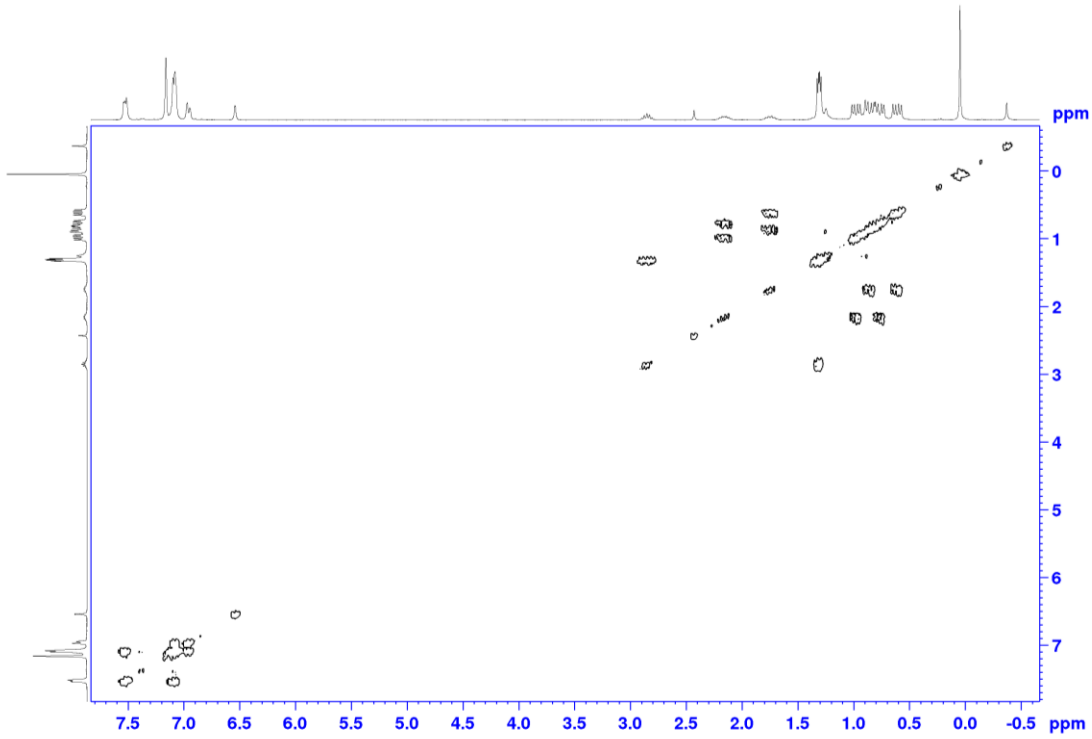

Figure S19. ^{1}H–^{1}H COSY NMR Spectrum of $L^{iPr}Lu(CH_2SiMe_3)(NHCPh_3)$ in benzene-d_6 at ambient temperature.

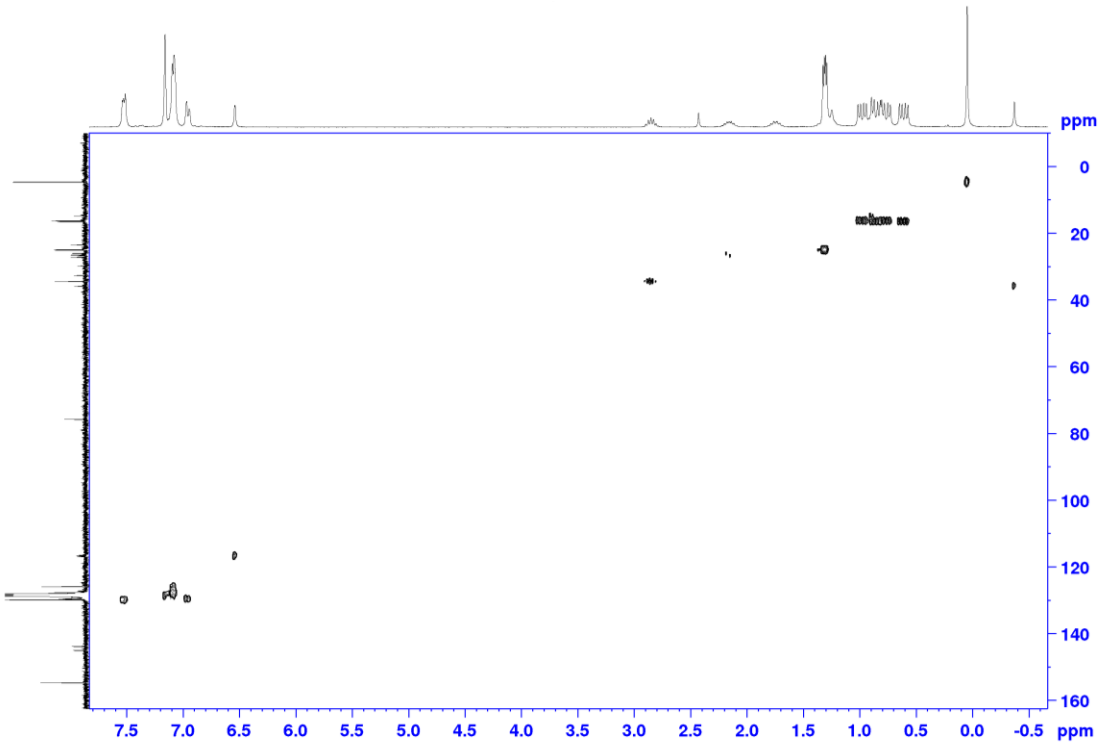

Figure S20. ^{1}H–^{13}C HSQC NMR Spectrum of $L^{iPr}Lu(CH_2SiMe_3)(NHCPh_3)$ in benzene-d_6 at ambient temperature.

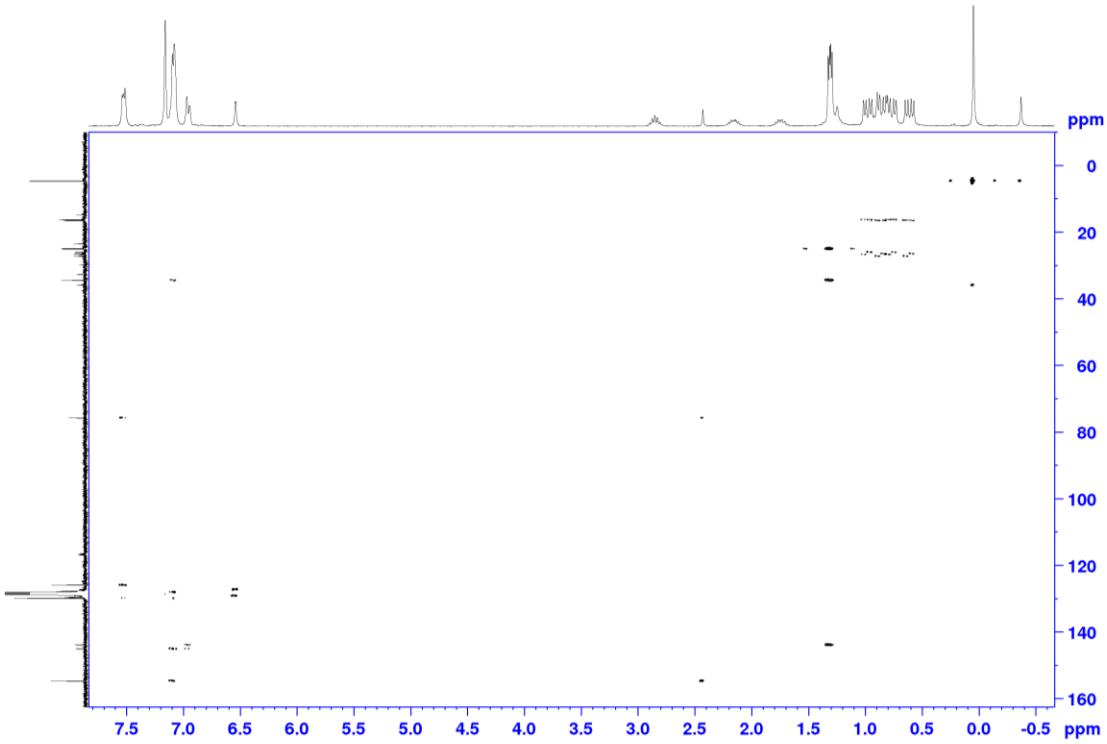

Figure S21. ^{1}H–^{13}C HMBC NMR Spectrum of $L^{iPr}Lu(CH_2SiMe_3)(NHCPh_3)$ in benzene-d_6 at ambient temperature.

$L^{iPr}Lu(CH_2SiMe_3)(NHDipp)$ (**7_{Dipp}**):

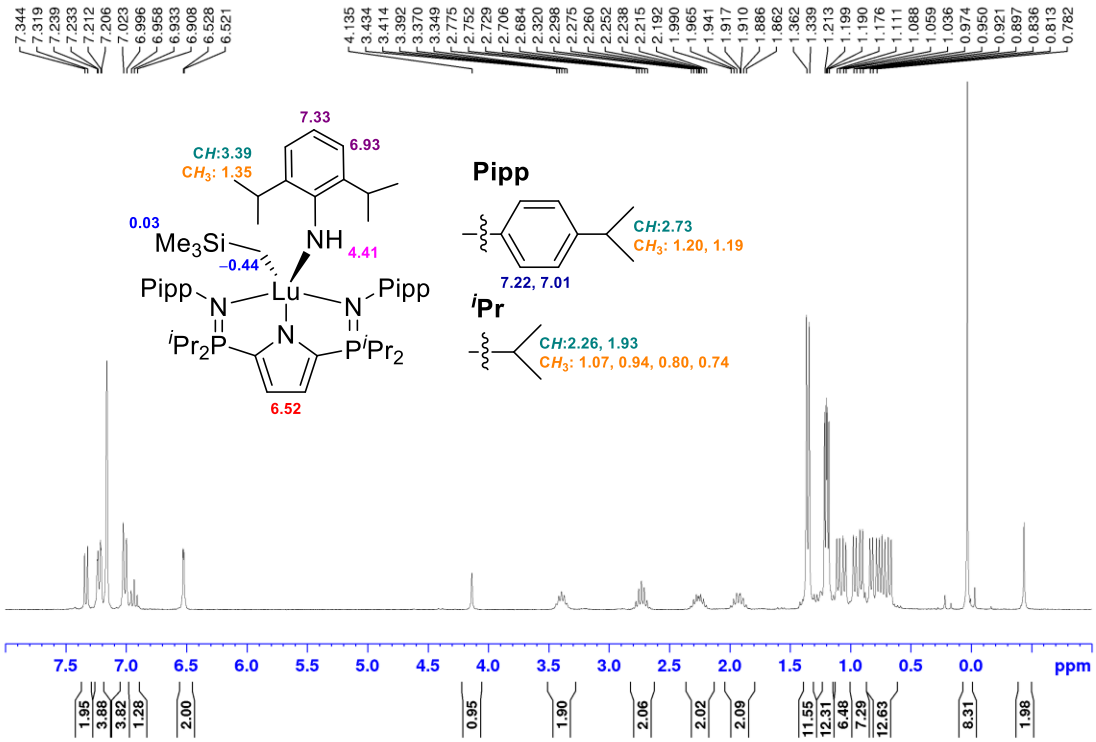

Figure S22. ^{1}H NMR Spectrum of $L^{iPr}Lu(CH_2SiMe_3)(NHDipp)$ in benzene-d_6 at ambient temperature.

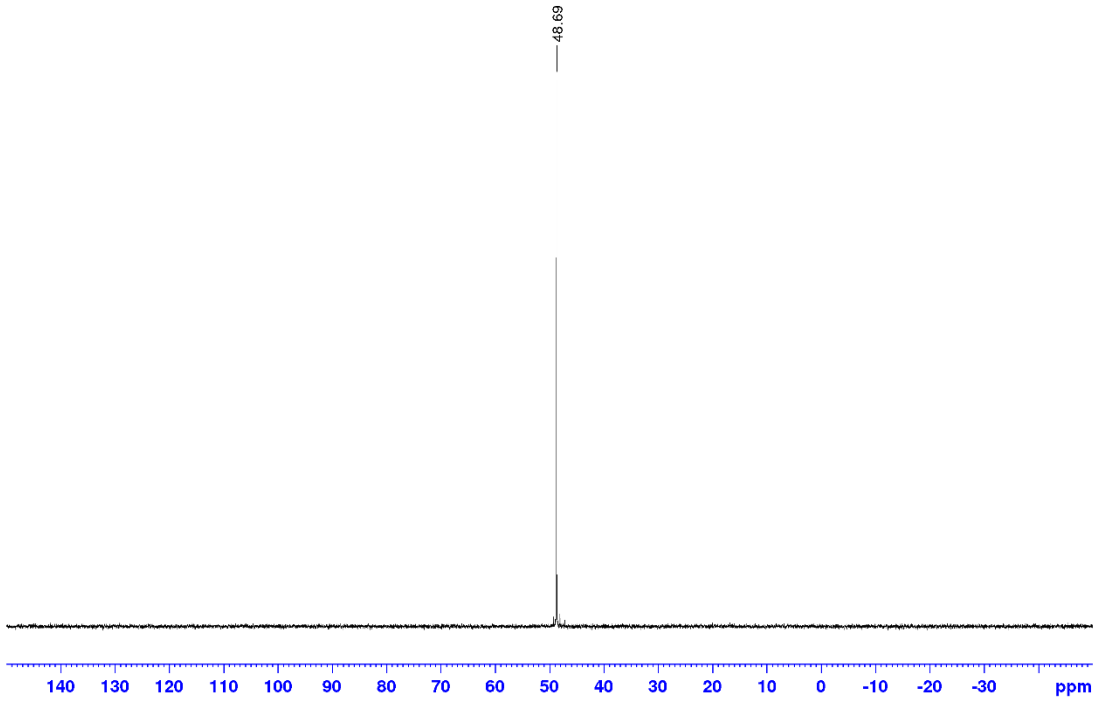

Figure S23. $^{31}P\{^{1}H\}$ NMR Spectrum of $L^{iPr}Lu(CH_2SiMe_3)(NHDipp)$ in benzene-d_6 at ambient temperature.

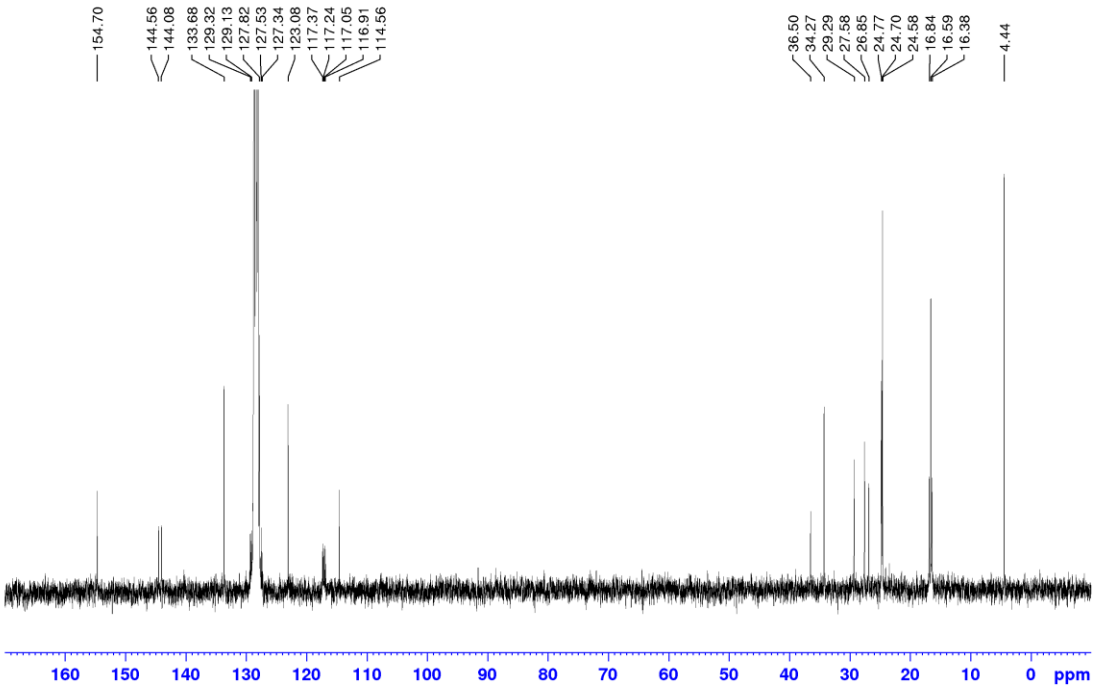

Figure S24. $^{13}C\{^{1}H\}$ NMR Spectrum of $L^{iPr}Lu(CH_2SiMe_3)(NHDipp)$ in benzene-d_6 at ambient temperature.

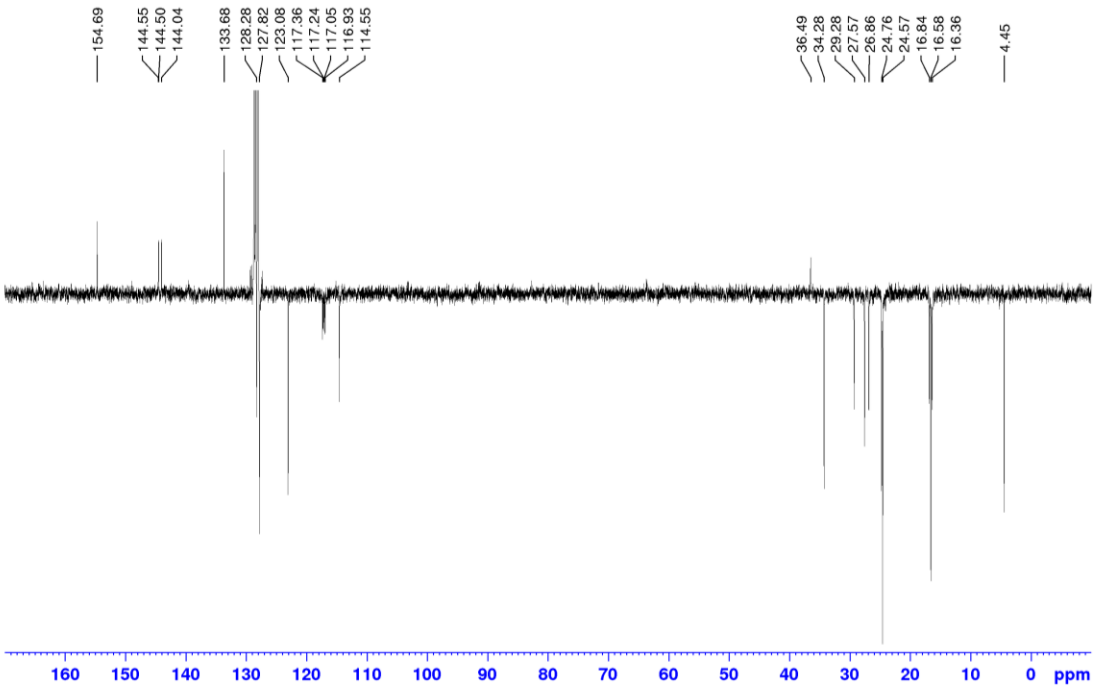

Figure S25. APT NMR Spectrum of $L^{iPr}Lu(CH_2SiMe_3)(NHDipp)$ in benzene-d_6 at ambient temperature.

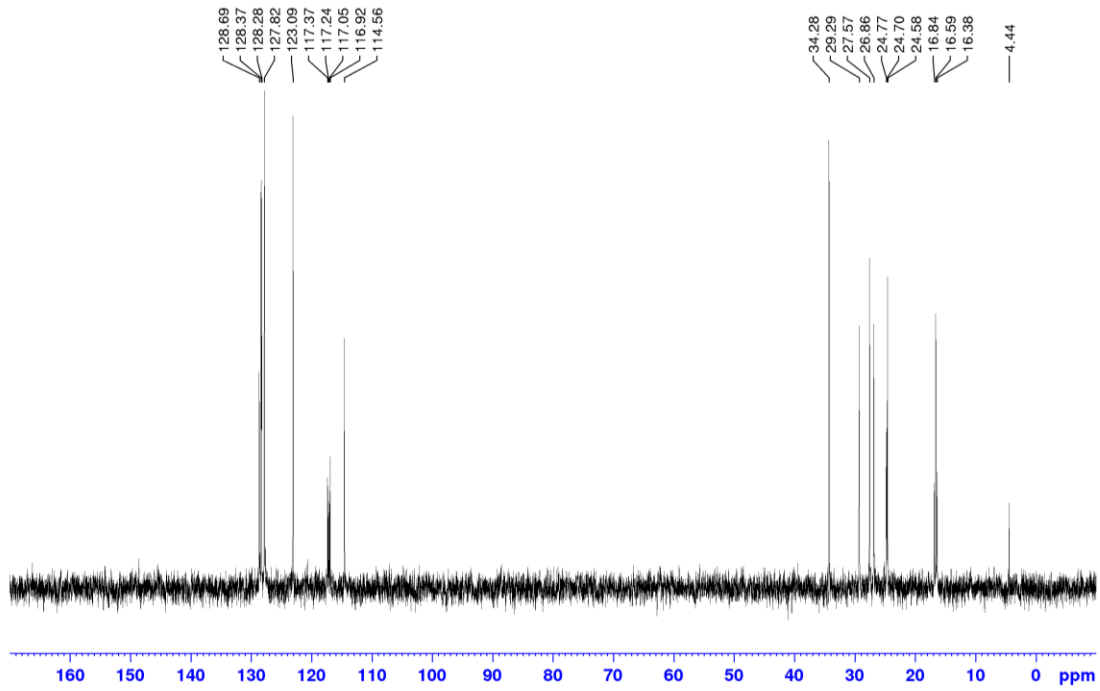

Figure S26. DEPT-135 NMR Spectrum of $L^{iPr}Lu(CH_2SiMe_3)(NHDipp)$ in benzene-d_6 at ambient temperature.

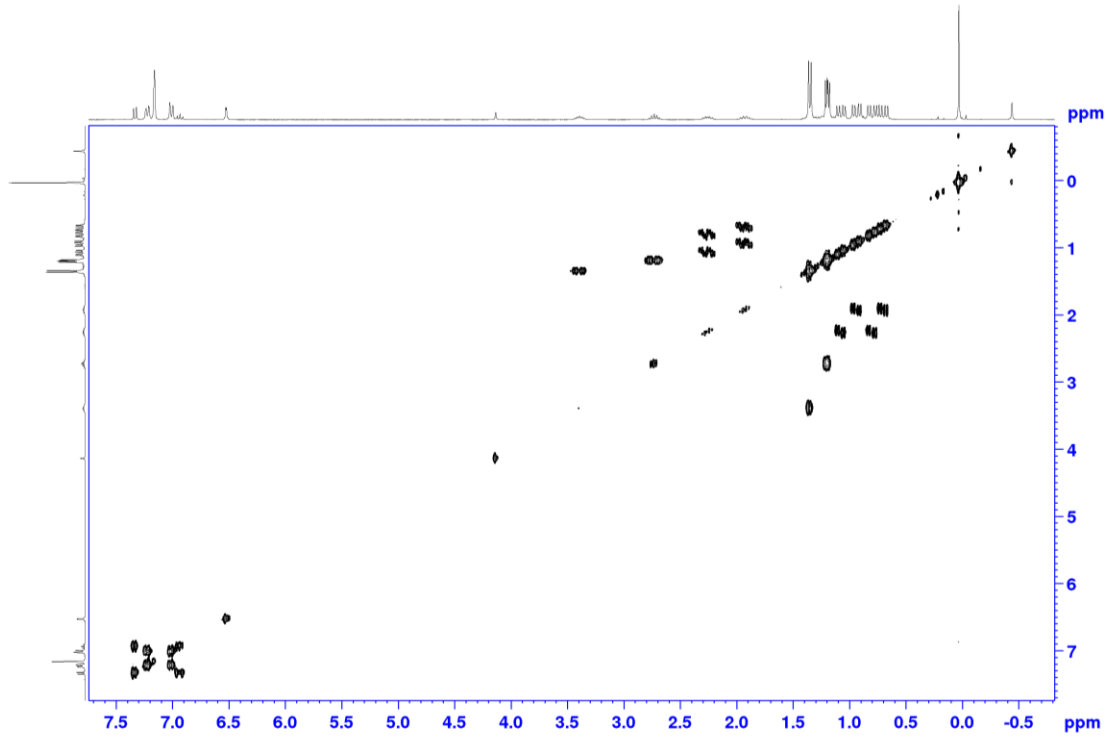

Figure S27. ^1H–^1H COSY NMR Spectrum of $L^{iPr}Lu(CH_2SiMe_3)(NHDipp)$ in benzene-d_6 at ambient temperature.

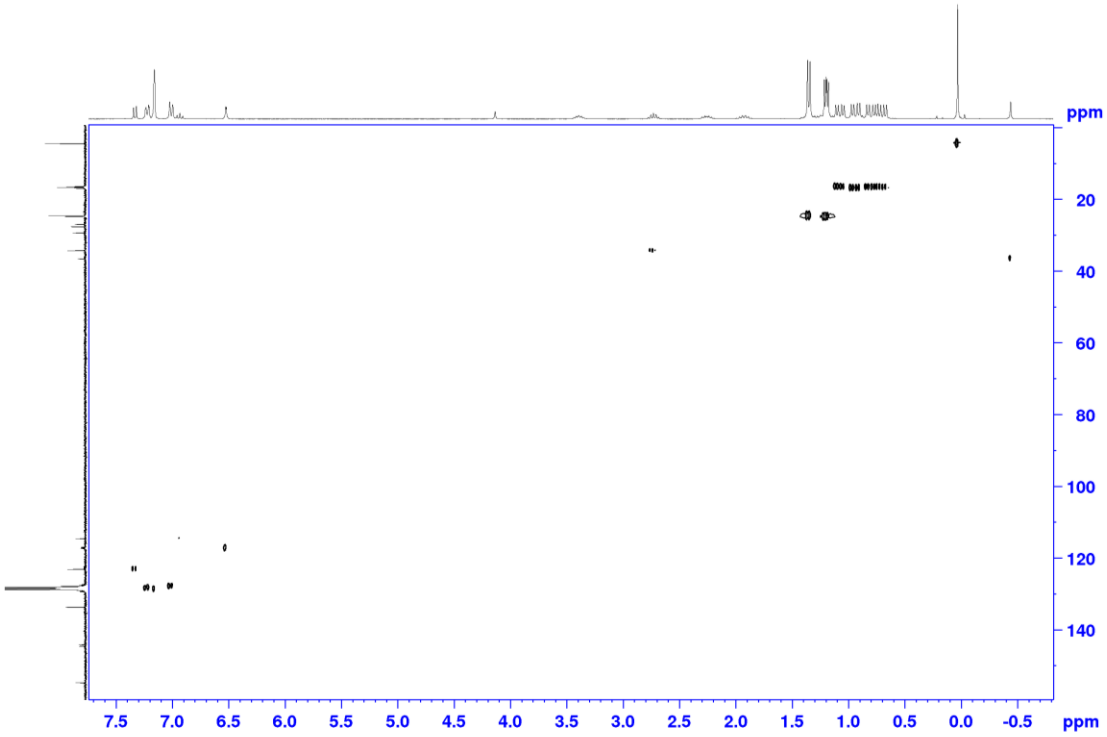

Figure S28. ^{1}H–^{13}C HSQC NMR Spectrum of $L^{iPr}Lu(CH_2SiMe_3)(NHDipp)$ in benzene-d_6 at ambient temperature.

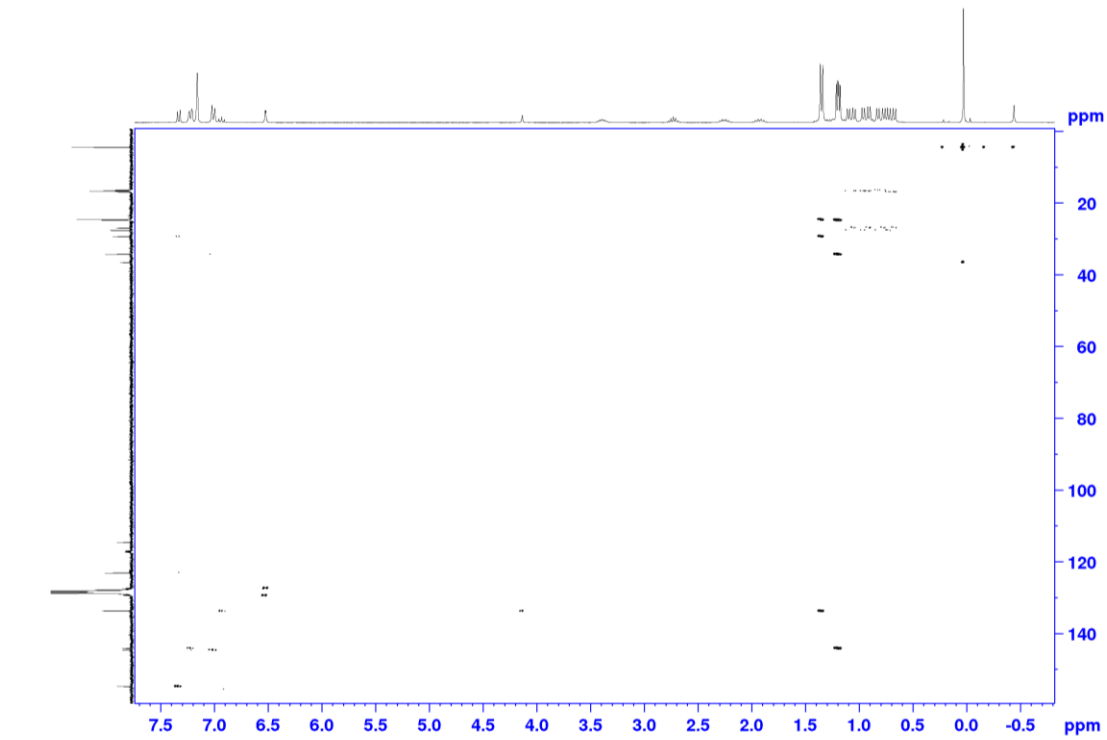

Figure S29. ^{1}H–^{13}C HMBC NMR Spectrum of $L^{iPr}Lu(CH_2SiMe_3)(NHDipp)$ in benzene-d_6 at ambient temperature.

$L^{iPr}Lu(NHCPh_3)_2$ (**8_{CPh3}**):

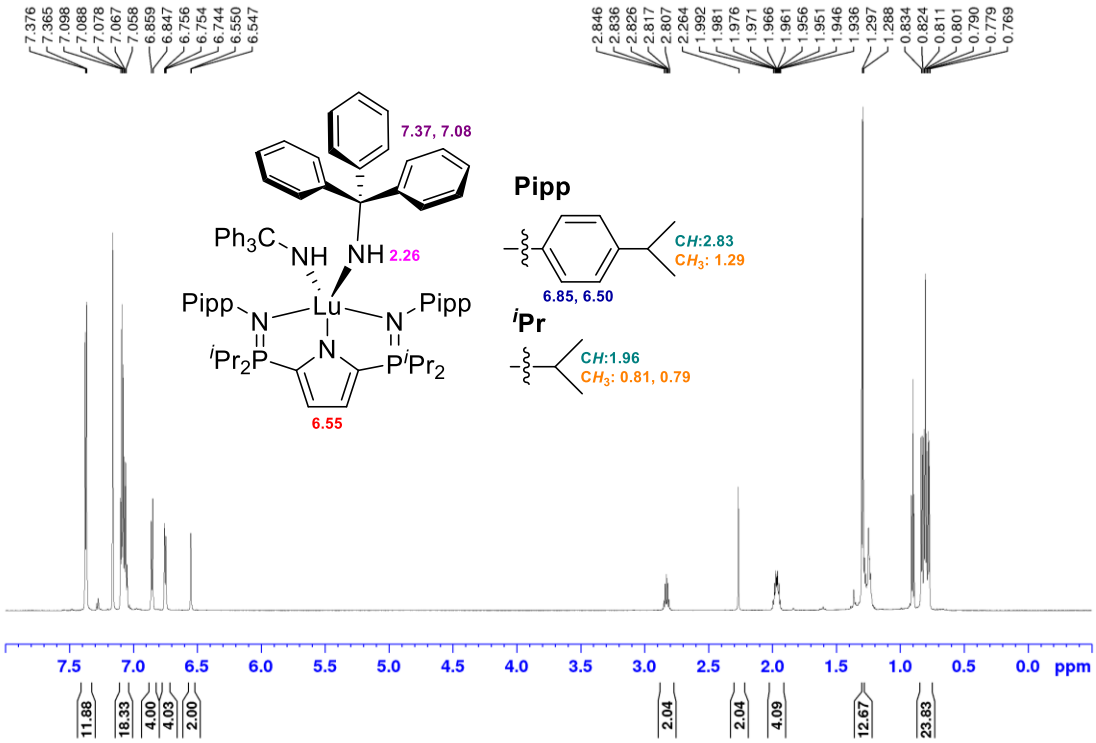

Figure S30 ^{1}H NMR spectrum of $L^{iPr}Lu(NHCPh_3)_2$ in benzene-d_6 at ambient temperature.

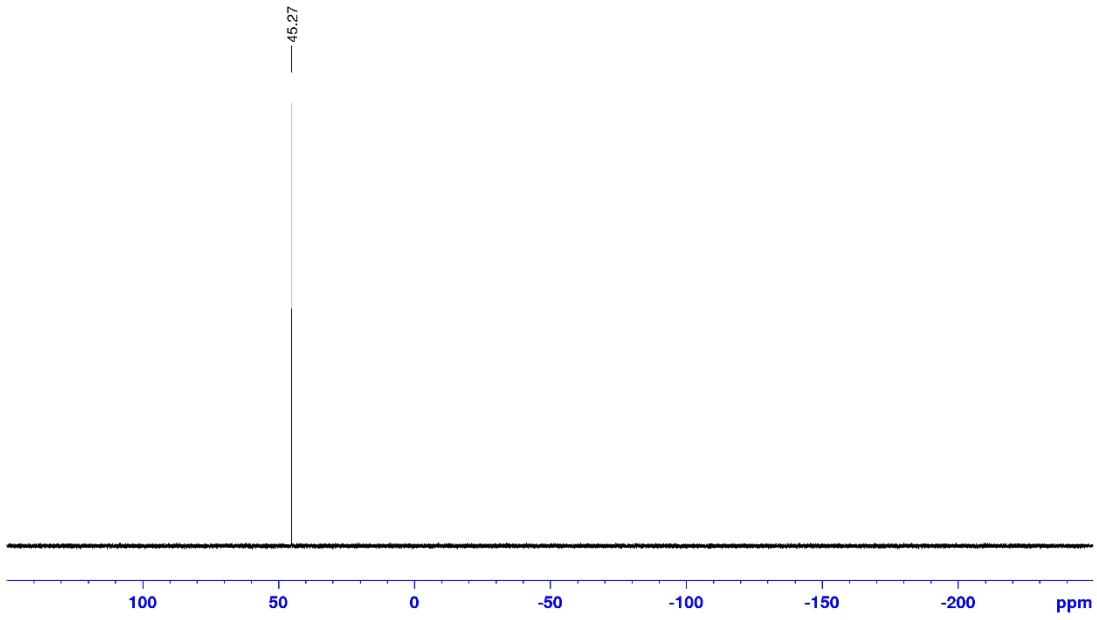

Figure S31 $^{31}P\{^{1}H\}$ NMR spectrum of $L^{iPr}Lu(NHCPh_3)_2$ in benzene-d_6 at ambient temperature.

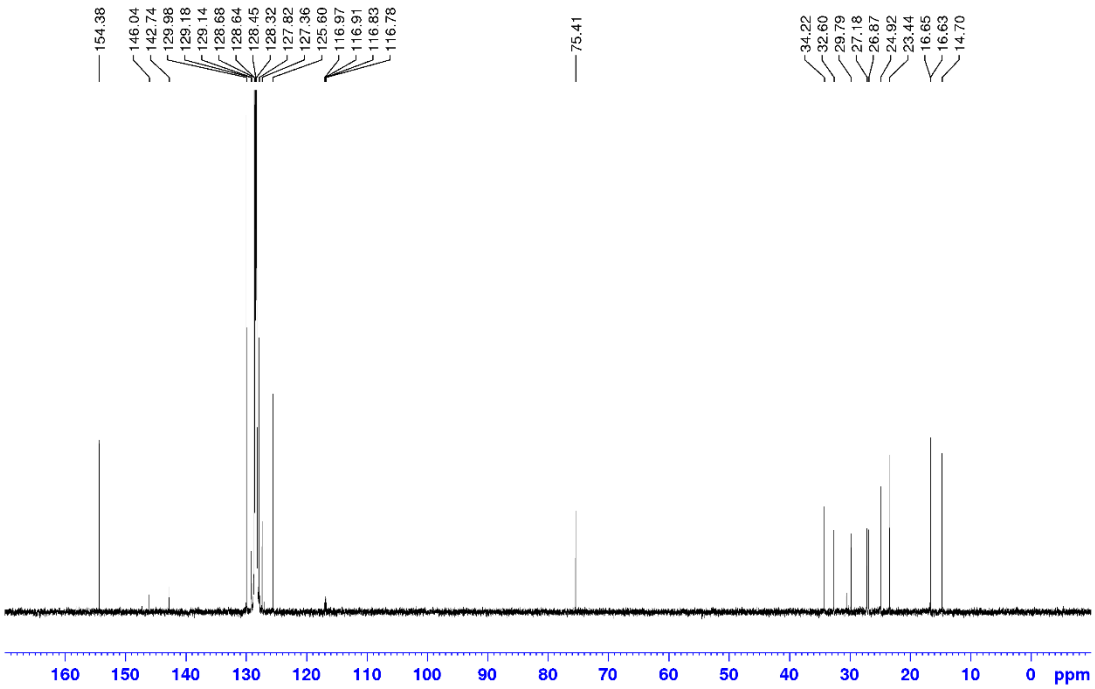

Figure S32 $^{13}C\{^{1}H\}$ NMR spectrum of $L^{iPr}Lu(NHCPh_3)_2$ in benzene-d_6 at ambient temperature.

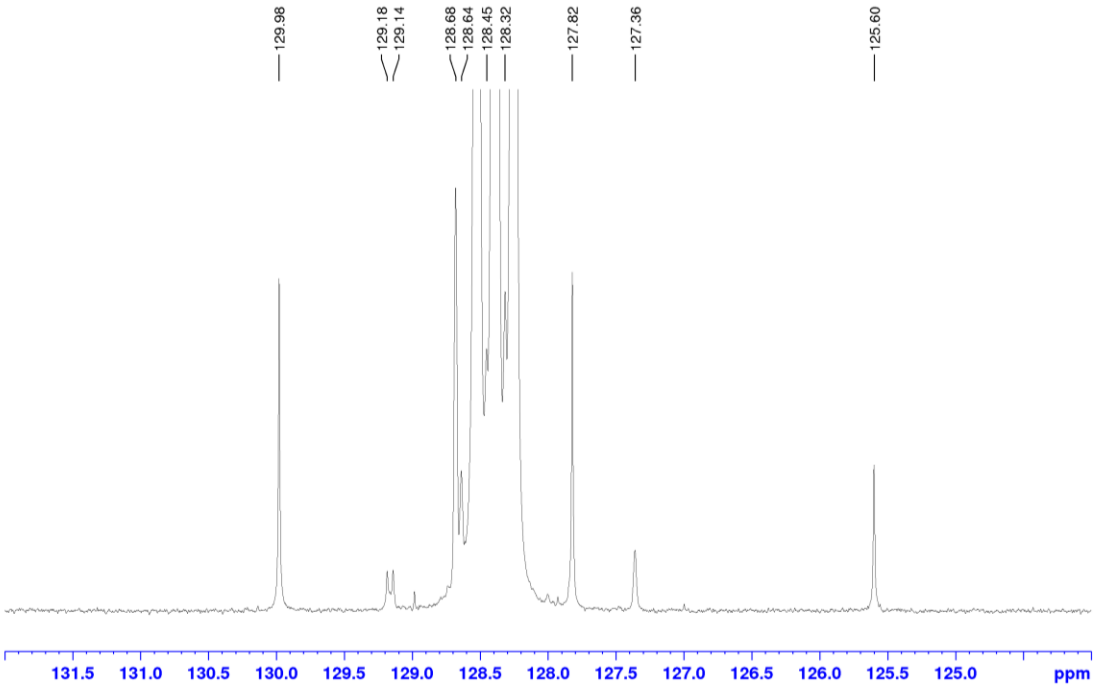

Figure S33 Aromatic Region of the $^{13}C\{^{1}H\}$ NMR spectrum of $L^{iPr}Lu(NHCPh_3)_2$ in benzene-d_6 at ambient temperature.

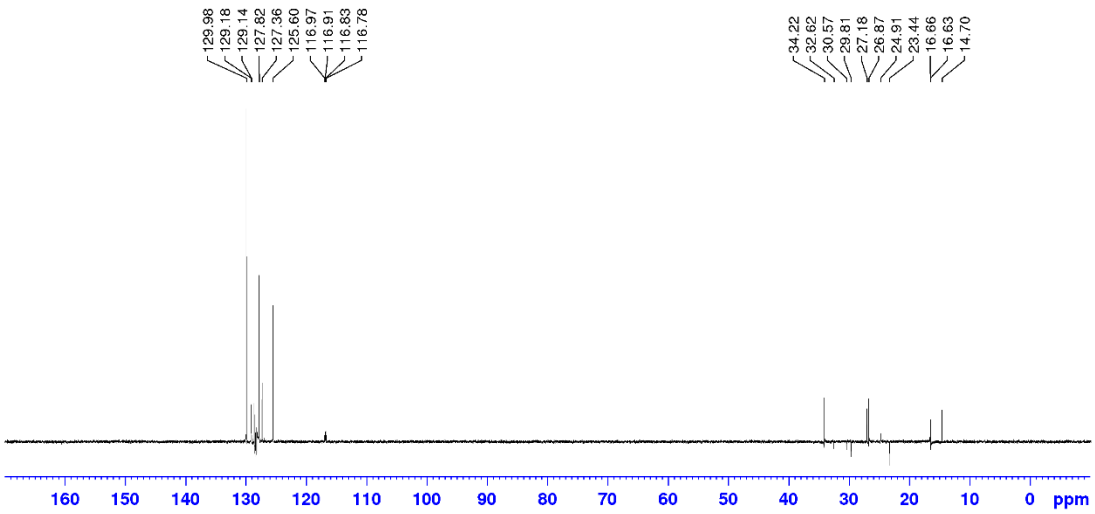

Figure S34 DEPT-135 NMR spectrum of $L^{iPr}Lu(NHCPh_3)_2$ in benzene-d_6 at ambient temperature.

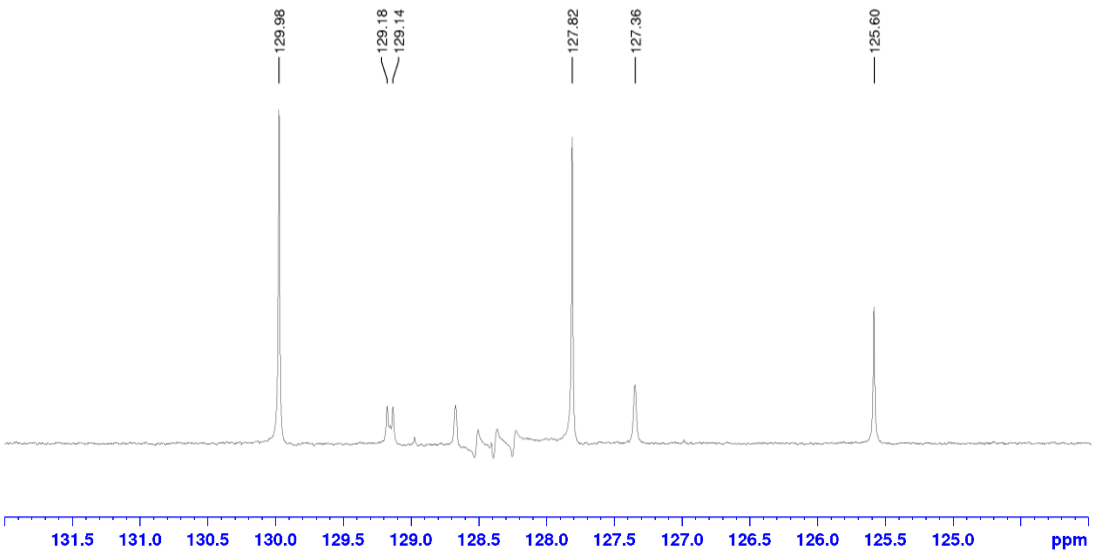

Figure S35 Aromatic Region of the DEPT-135 NMR spectrum of $L^{iPr}Lu(NHCPh_3)_2$ in benzene-d_6 at ambient temperature.

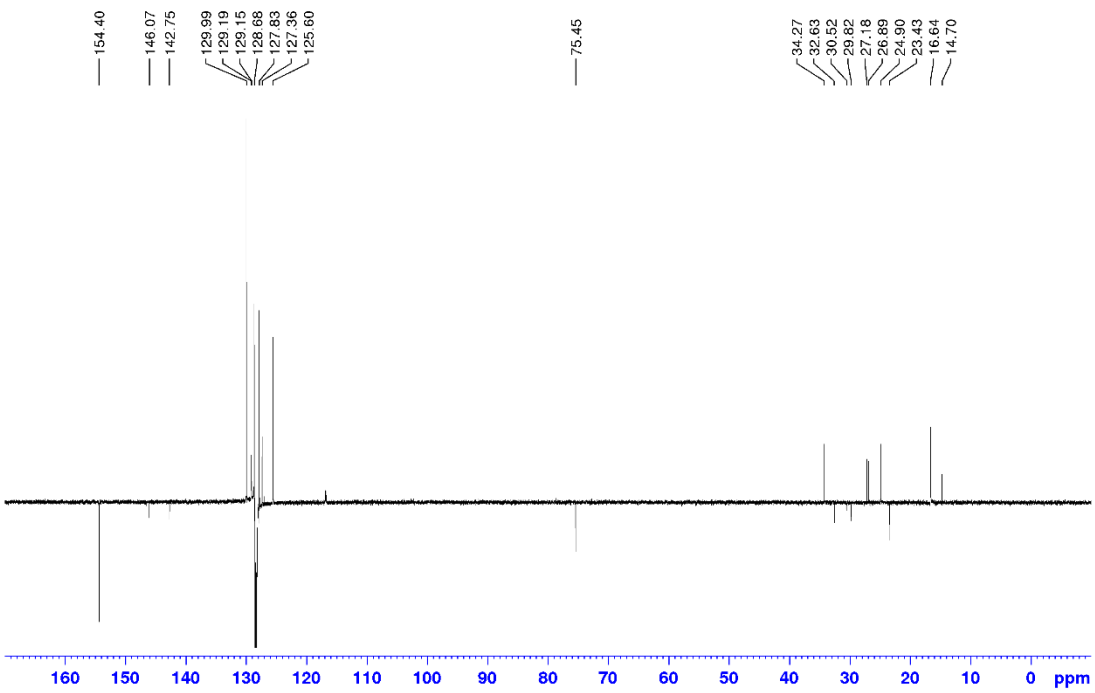

Figure S36 APT NMR spectrum of $L^{iPr}Lu(NHCPh_3)_2$ in benzene-d_6 at ambient temperature.

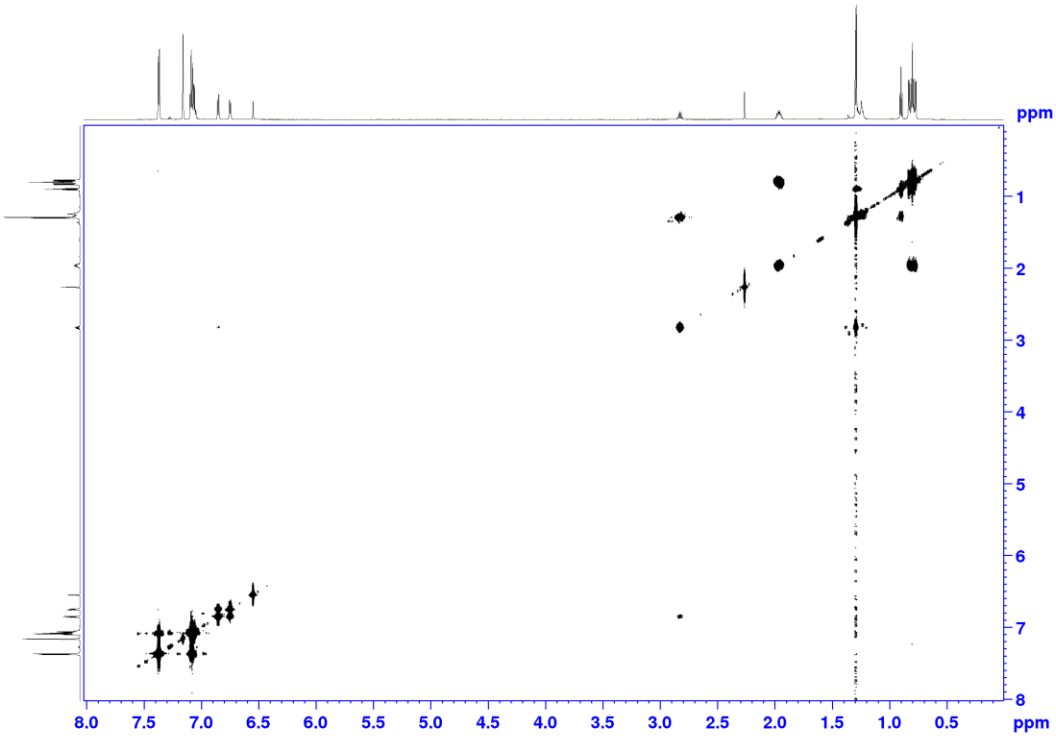

Figure S37 ^{1}H–^{1}H COSY NMR spectrum of $L^{iPr}Lu(NHCPh_3)_2$ in benzene-d_6 at ambient temperature.

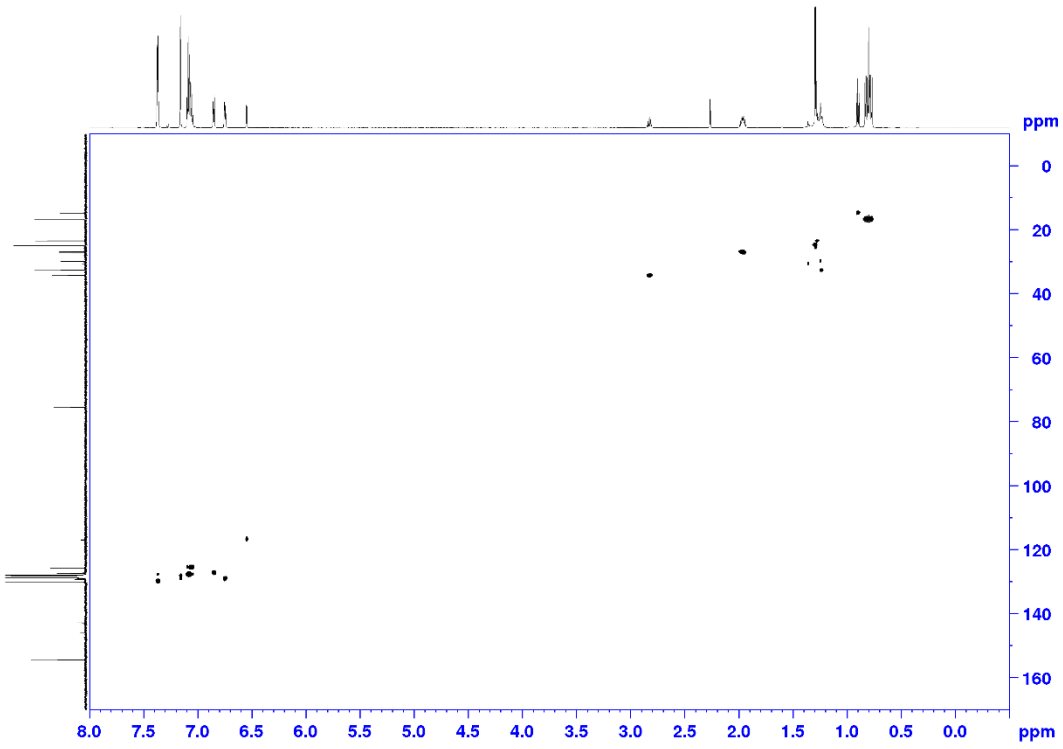

Figure S38 ^{1}H–^{13}C HSQC NMR spectrum of $L^{iPr}Lu(NHCPh_3)_2$ in benzene-d_6 at ambient temperature.

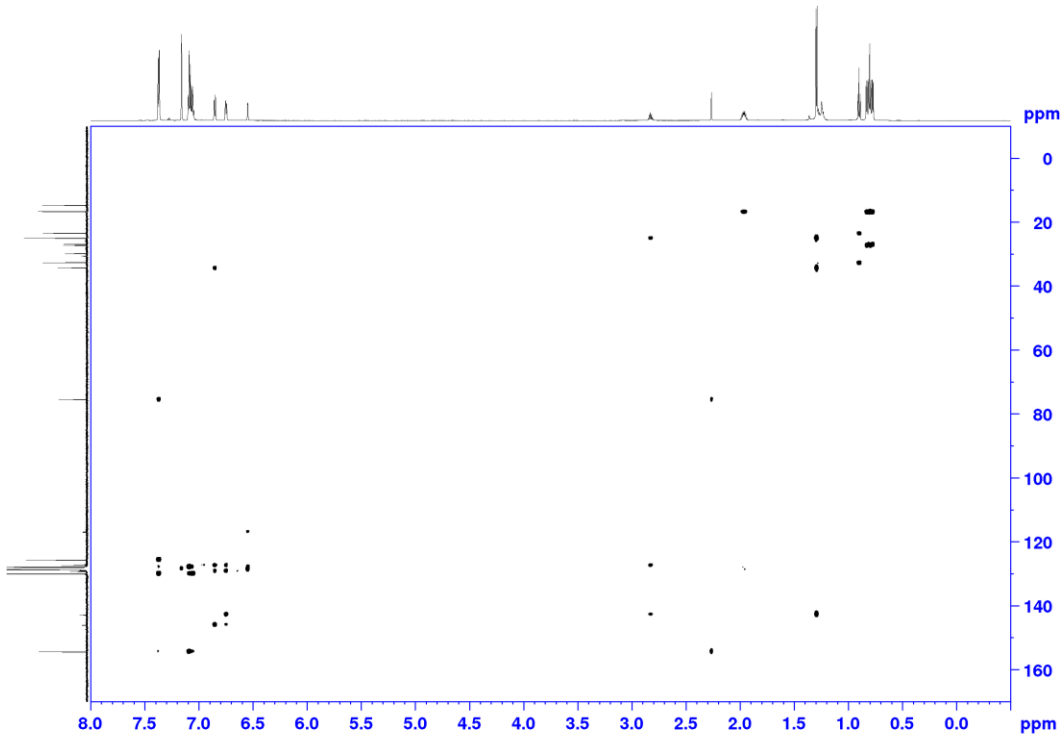

Figure S39 ^{1}H–^{13}C HMBC NMR spectrum of $L^{iPr}Lu(NHCPh_3)_2$ in benzene-d_6 at ambient temperature.

$L^{iPr}Lu(NHDipp)_2$ (**8$_{Dipp}$**):

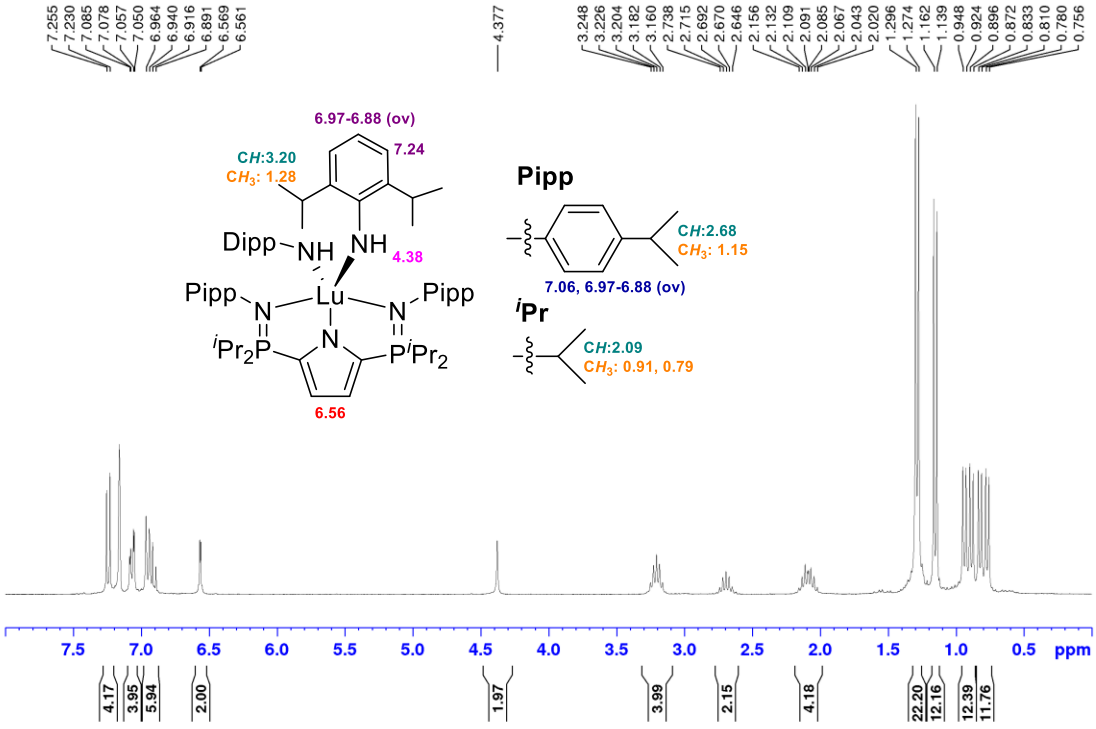

Figure S40. ^{1}H NMR Spectrum of $L^{iPr}Lu(NHDipp)_2$ in benzene-d_6 at ambient temperature.

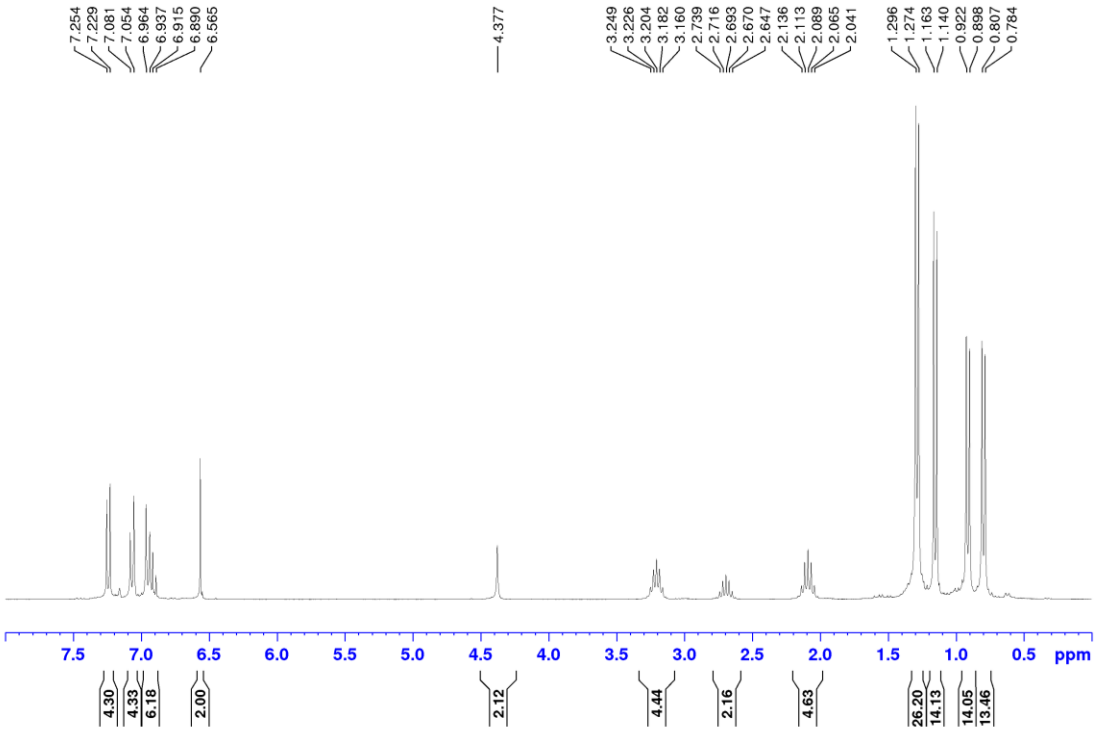

Figure S41. ^{1}H{^{31}P} NMR Spectrum of $L^{iPr}Lu(NHDipp)_2$ in benzene-d_6 at ambient temperature.

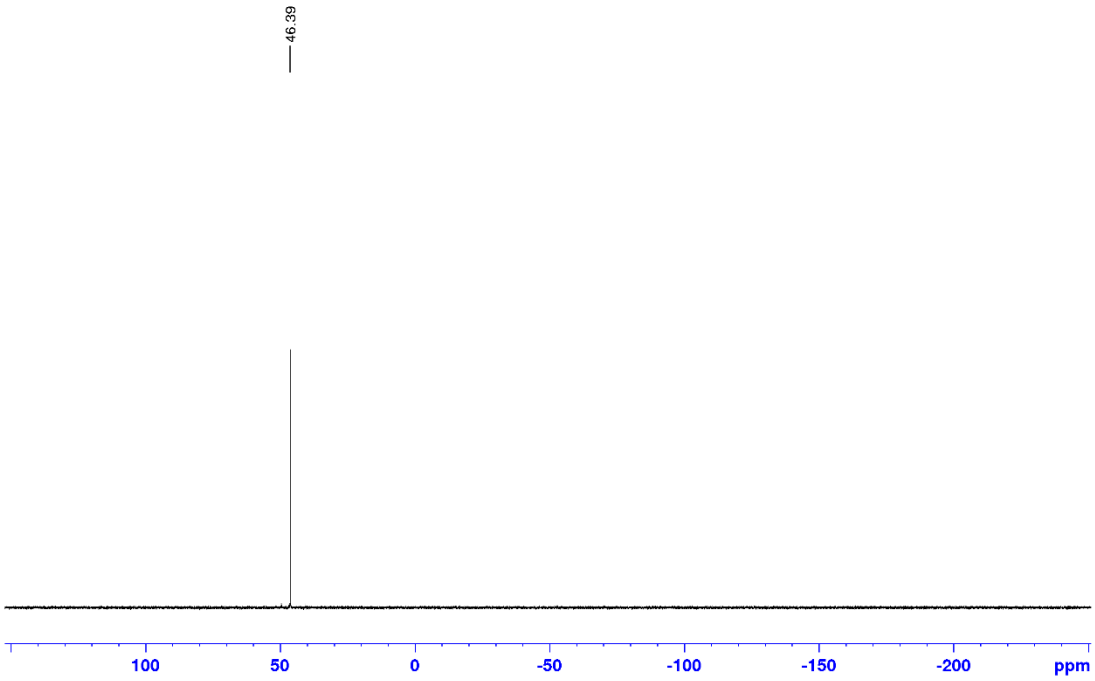

Figure S42. $^{31}P\{^{1}H\}$ NMR Spectrum of $L^{iPr}Lu(NHDipp)_2$ in benzene-d_6 at ambient temperature.

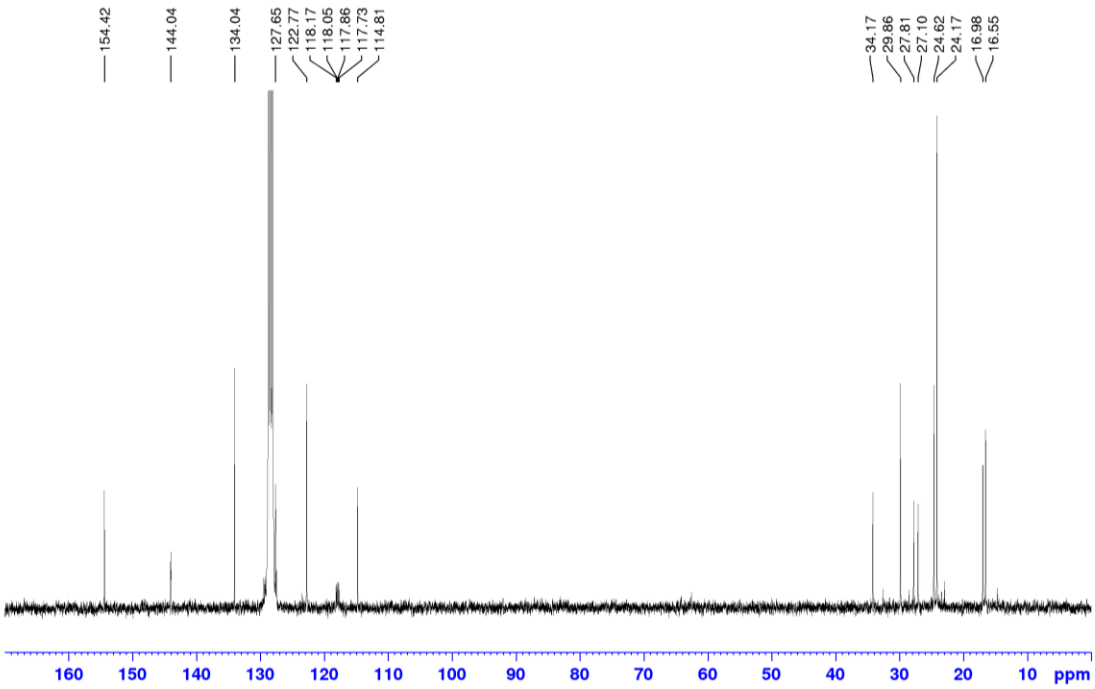

Figure S43. $^{13}C\{^{1}H\}$ NMR Spectrum of $L^{iPr}Lu(NHDipp)_2$ in benzene-d_6 at ambient temperature.

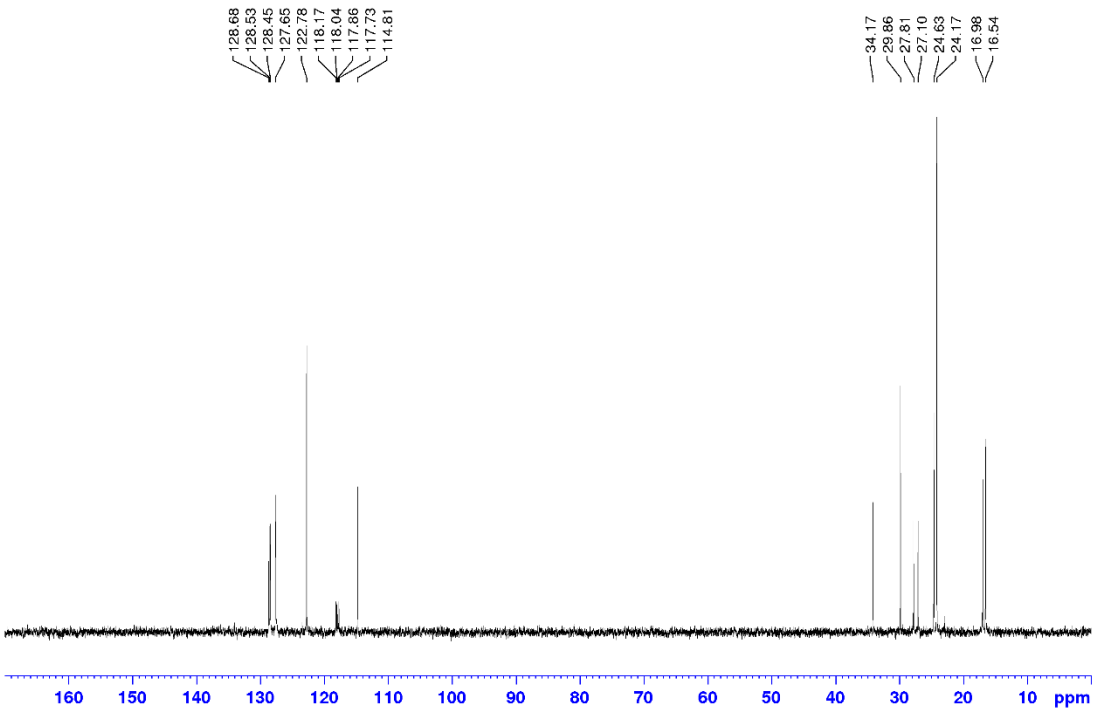

Figure S44. DEPT-135 NMR Spectrum of $L^{iPr}Lu(NHDipp)_2$ in benzene-d_6 at ambient temperature.

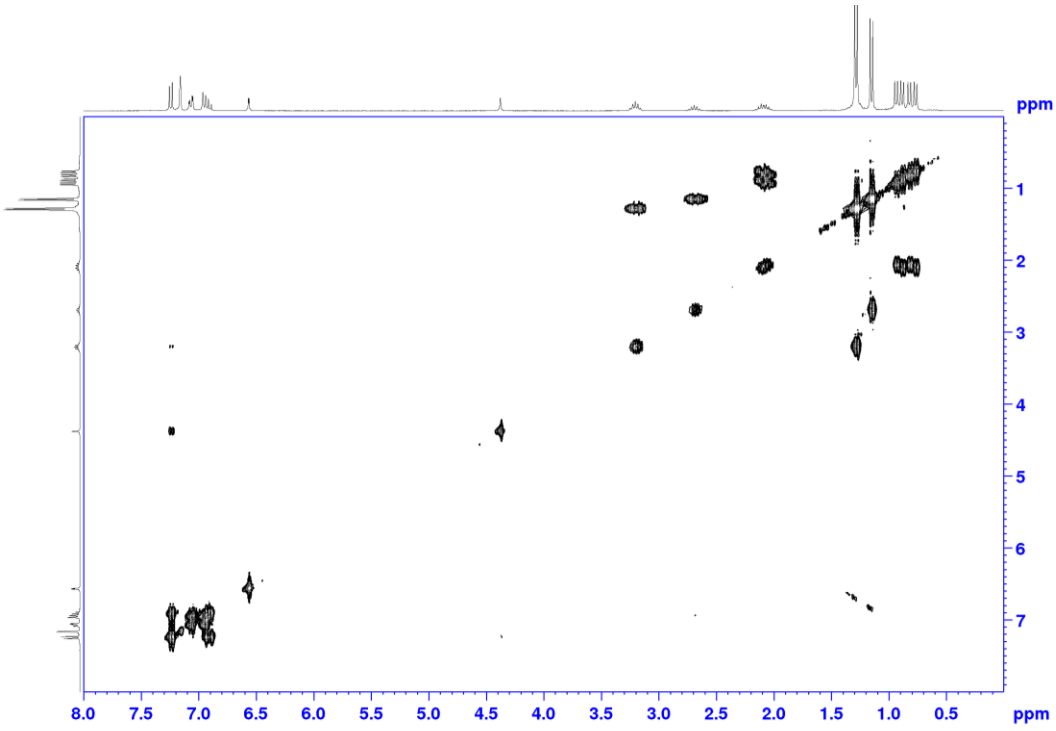

Figure S45. ^1H–^1H COSY NMR Spectrum of $L^{iPr}Lu(NHDipp)_2$ in benzene-d_6 at ambient temperature.

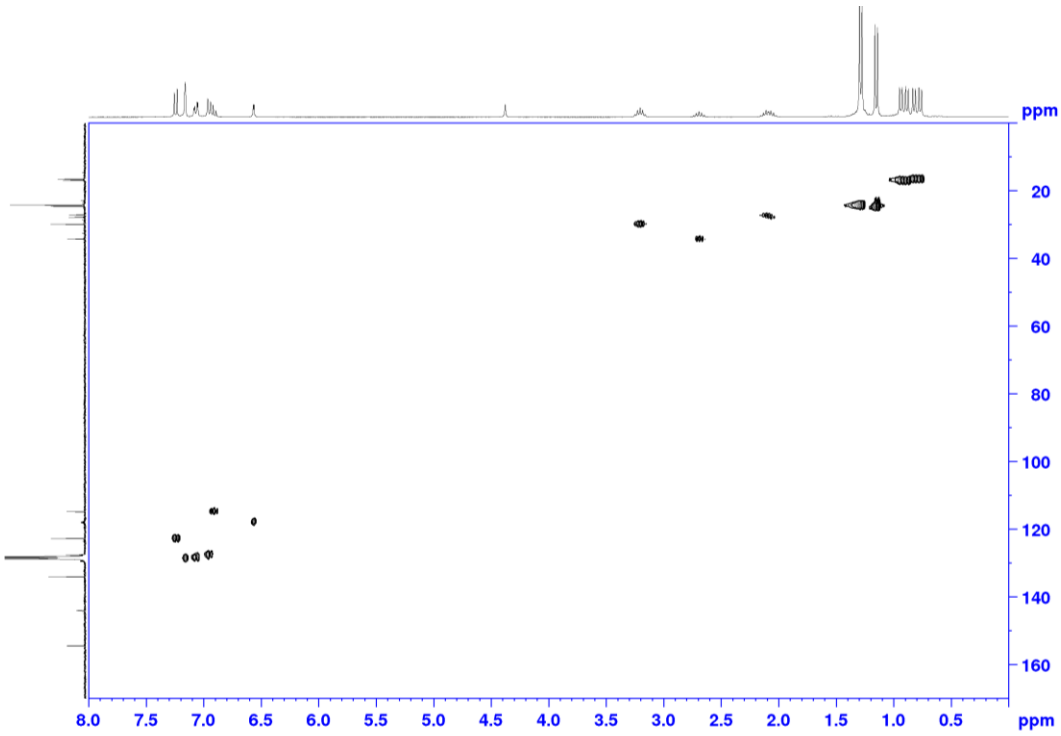

Figure S46. ^{1}H–^{13}C HSQC NMR Spectrum of $L^{iPr}Lu(NHDipp)_2$ in benzene-d_6 at ambient temperature.

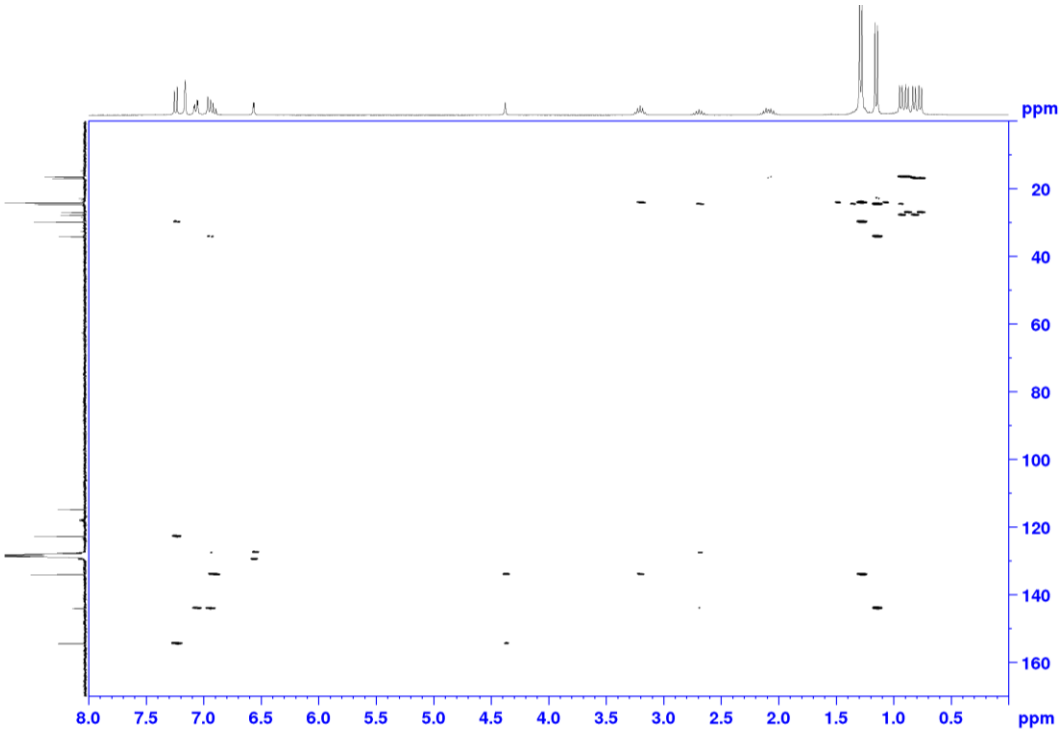

Figure S47. ^{1}H–^{13}C HMBC NMR Spectrum of $L^{iPr}Lu(NHDipp)_2$ in benzene-d_6 at ambient temperature.

HL^{Pm}(**11**):

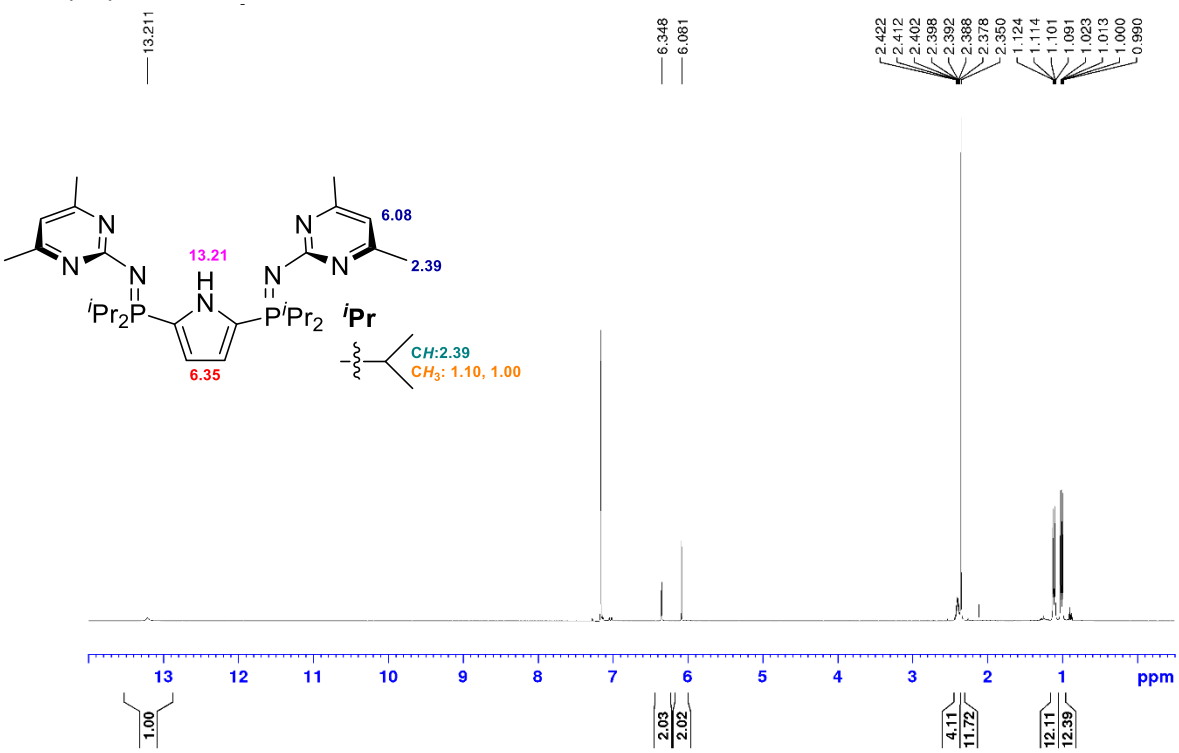

Figure S48. ^{1}H NMR Spectrum of HL^{Pm} in benzene-d_6 at ambient temperature.

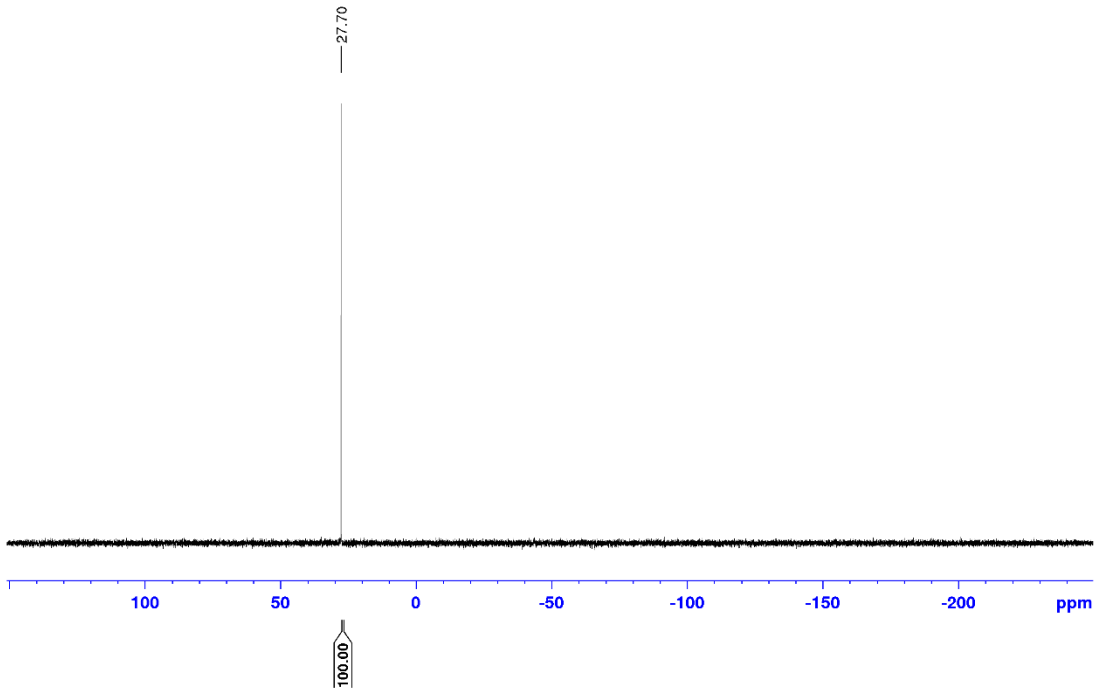

Figure S49. ^{31}P{^{1}H} NMR Spectrum of HL^{Pm} in benzene-d_6 at ambient temperature.

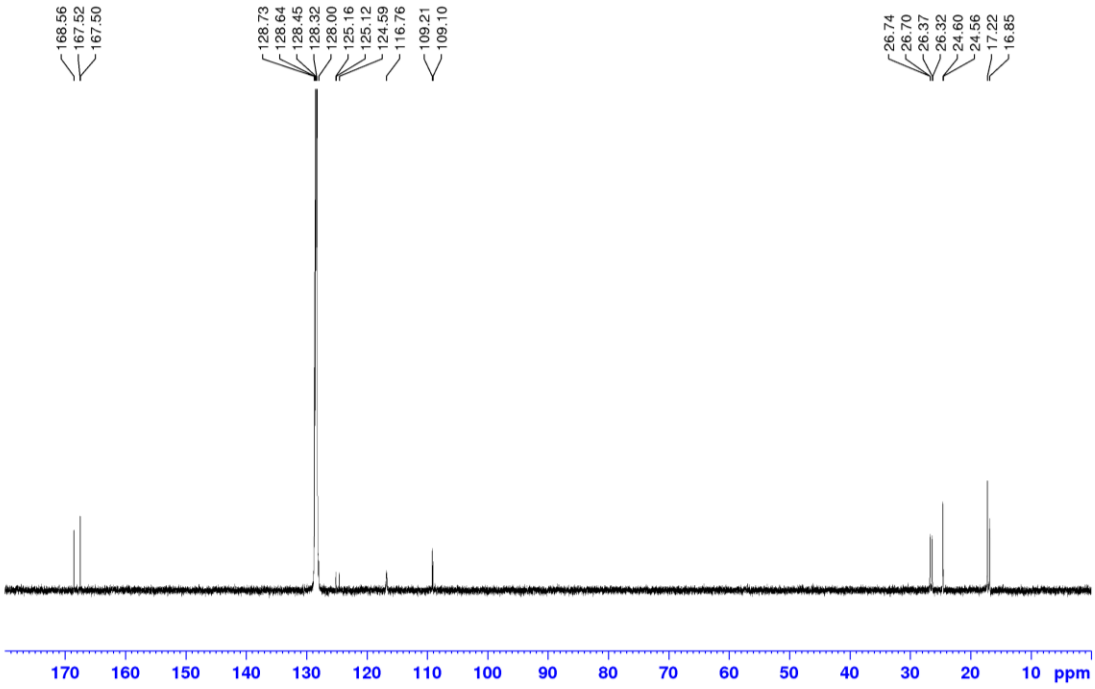

Figure S50. $^{13}C\{^{1}H\}$ NMR Spectrum of HL^{Pm} in benzene-d_6 at ambient temperature.

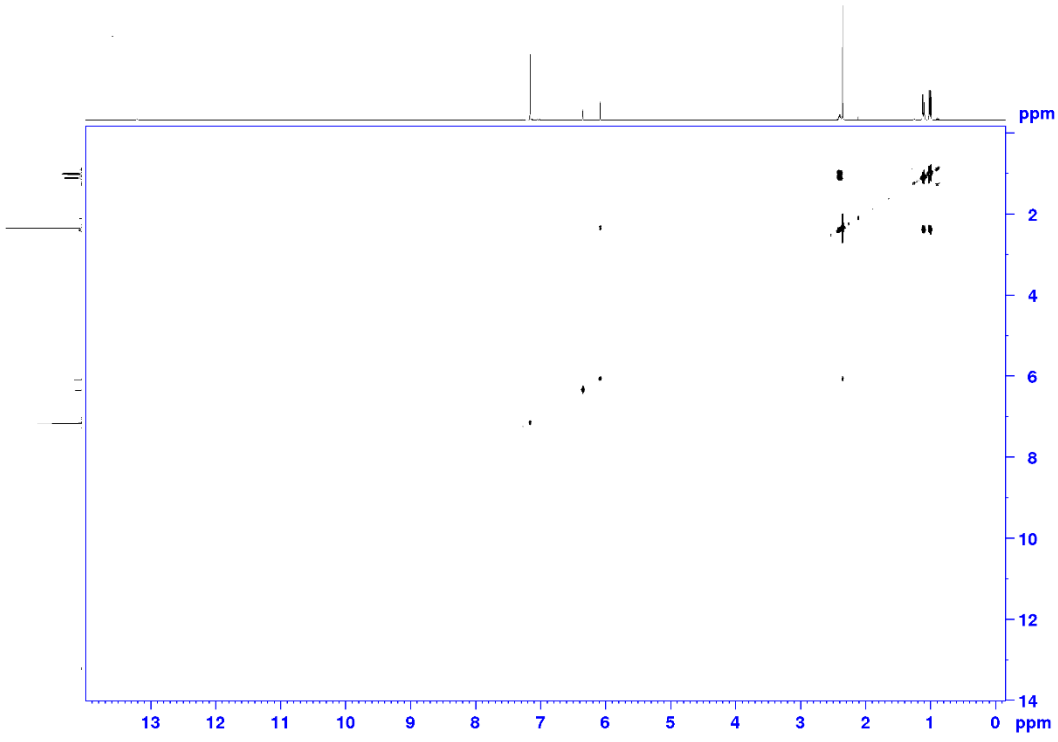

Figure S51. $^{1}H–^{1}H$ COSY NMR Spectrum of HL^{Pm} in benzene-d_6 at ambient temperature.

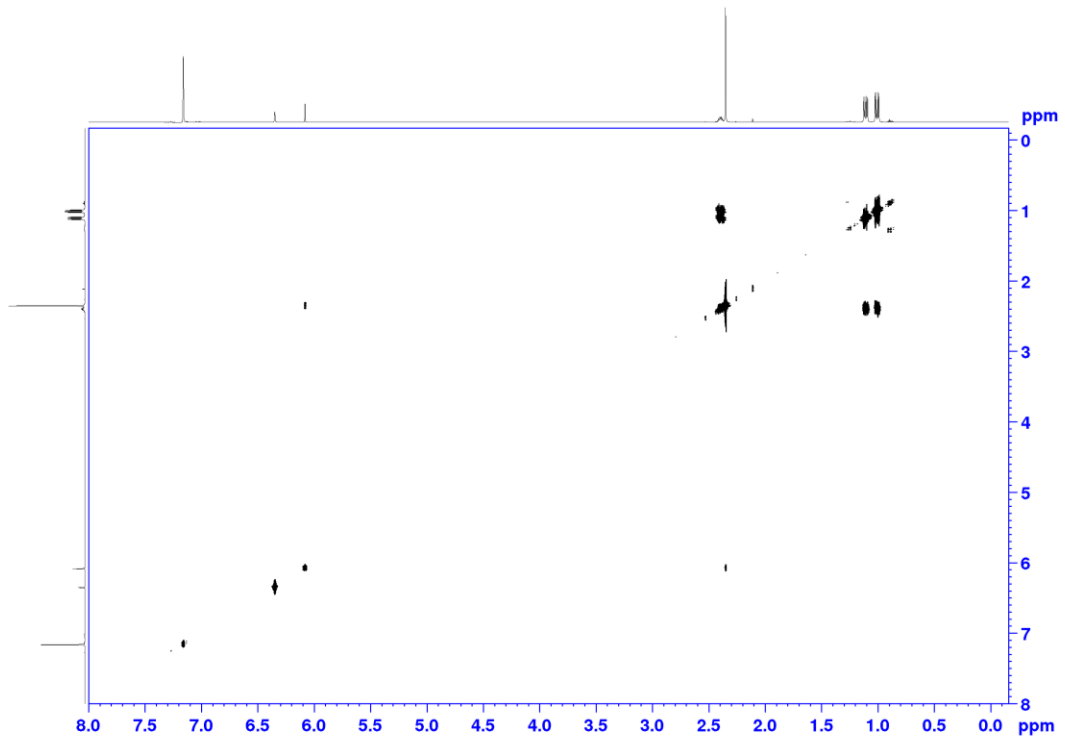

Figure S52. $^{1}H–^{1}H$ COSY NMR Spectrum of HL^{Pm} in benzene-d_6 at ambient temperature.

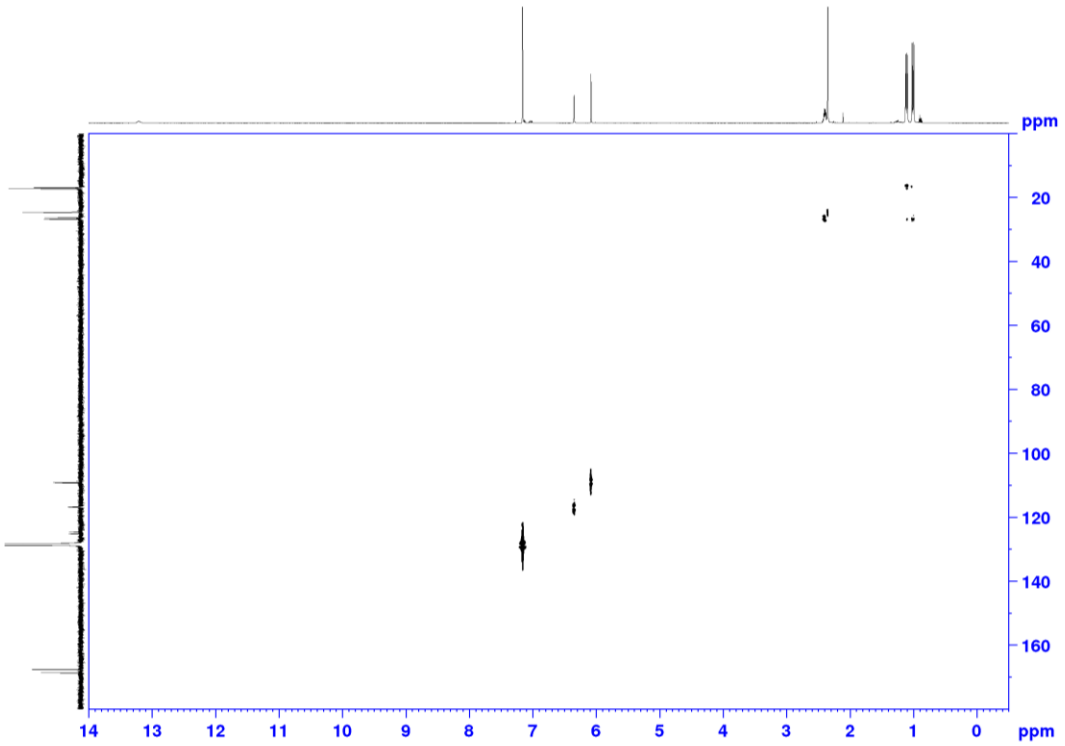

Figure S53. $^{1}H–^{13}C$ HSQC NMR Spectrum of HL^{Pm} in benzene-d_6 at ambient temperature.

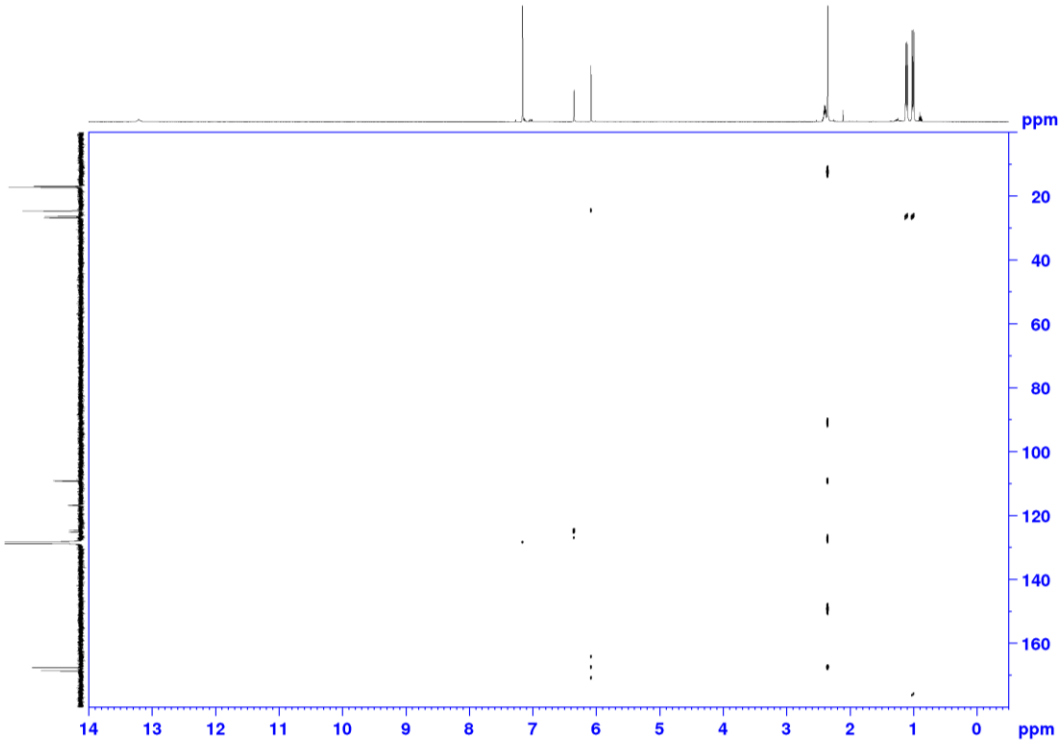

Figure S54. ^{1}H–^{13}C HMBC NMR Spectrum of HL^{Pm} in benzene-d_6 at ambient temperature.

$L^{Pm}Lu(CH_2SiMe_3)_2$ (**12**):

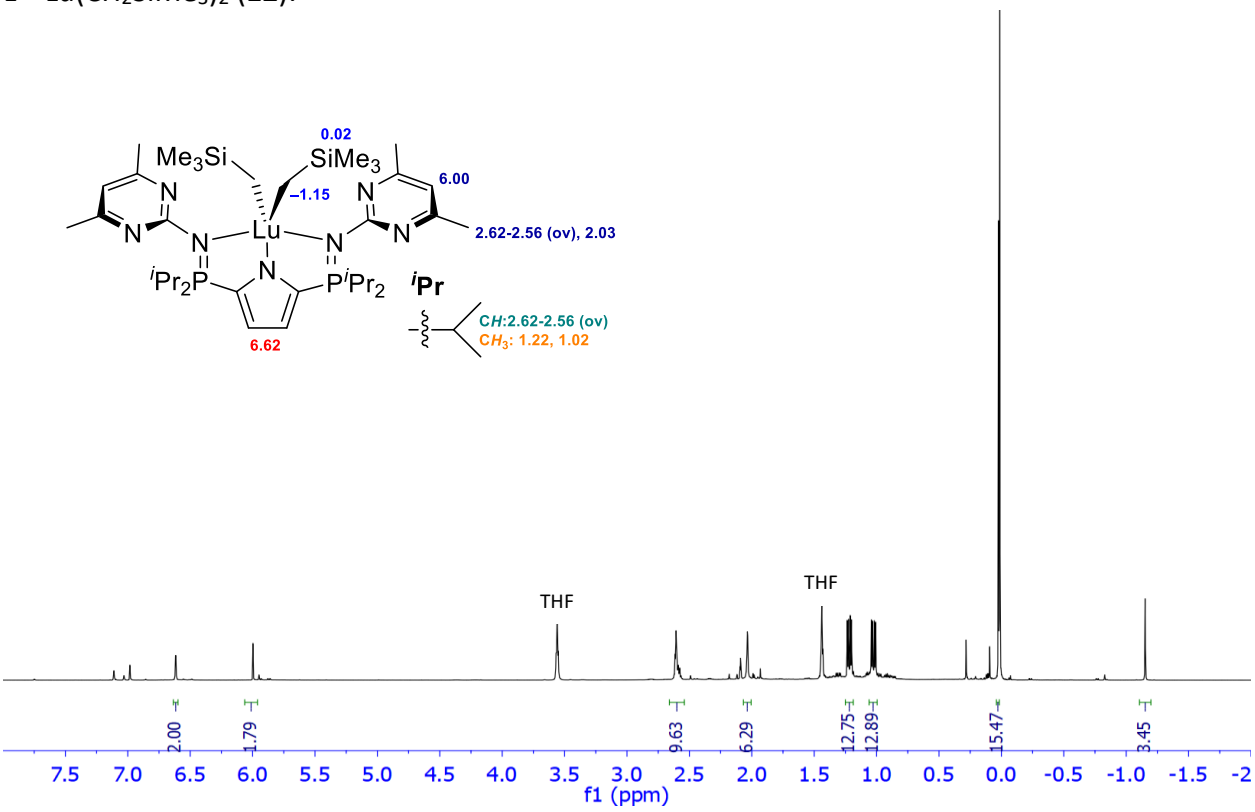

Figure S55. ^{1}H NMR Spectrum of $L^{Pm}Lu(CH_2SiMe_3)_2$ in toluene-d_8 at ambient temperature.

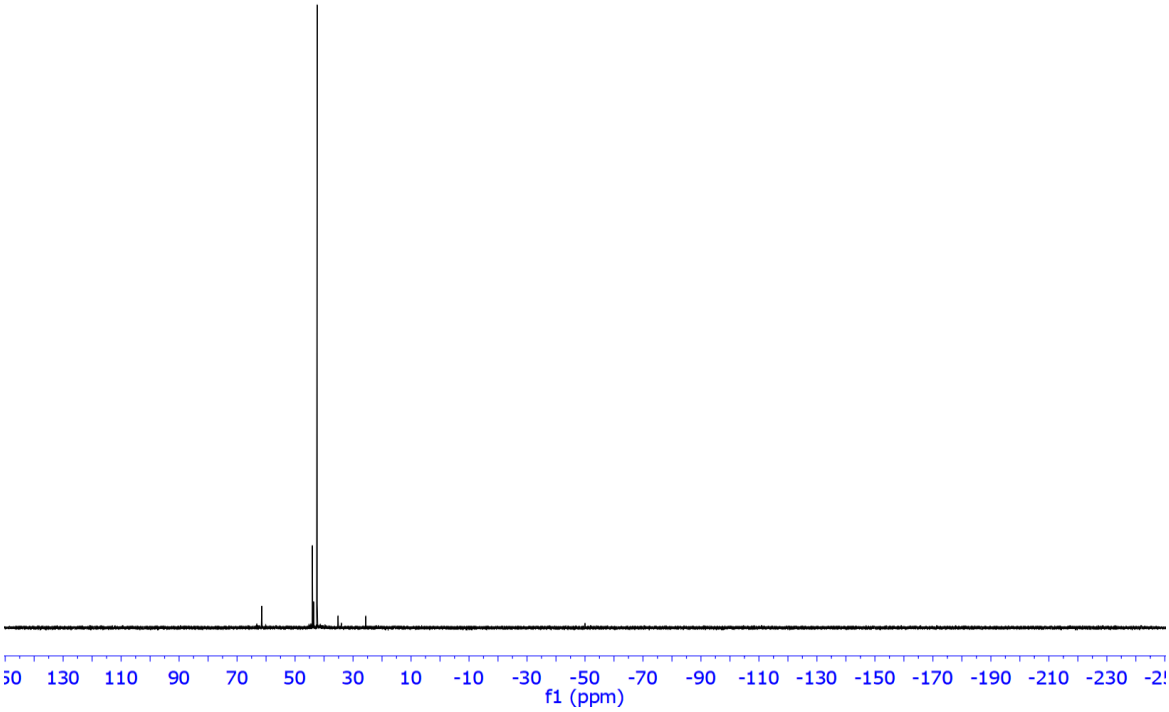

Figure S56. $^{31}P\{^{1}H\}$ NMR Spectrum of $L^{Pm}Lu(CH_2SiMe_3)_2$ in toluene-d_8 at ambient temperature.

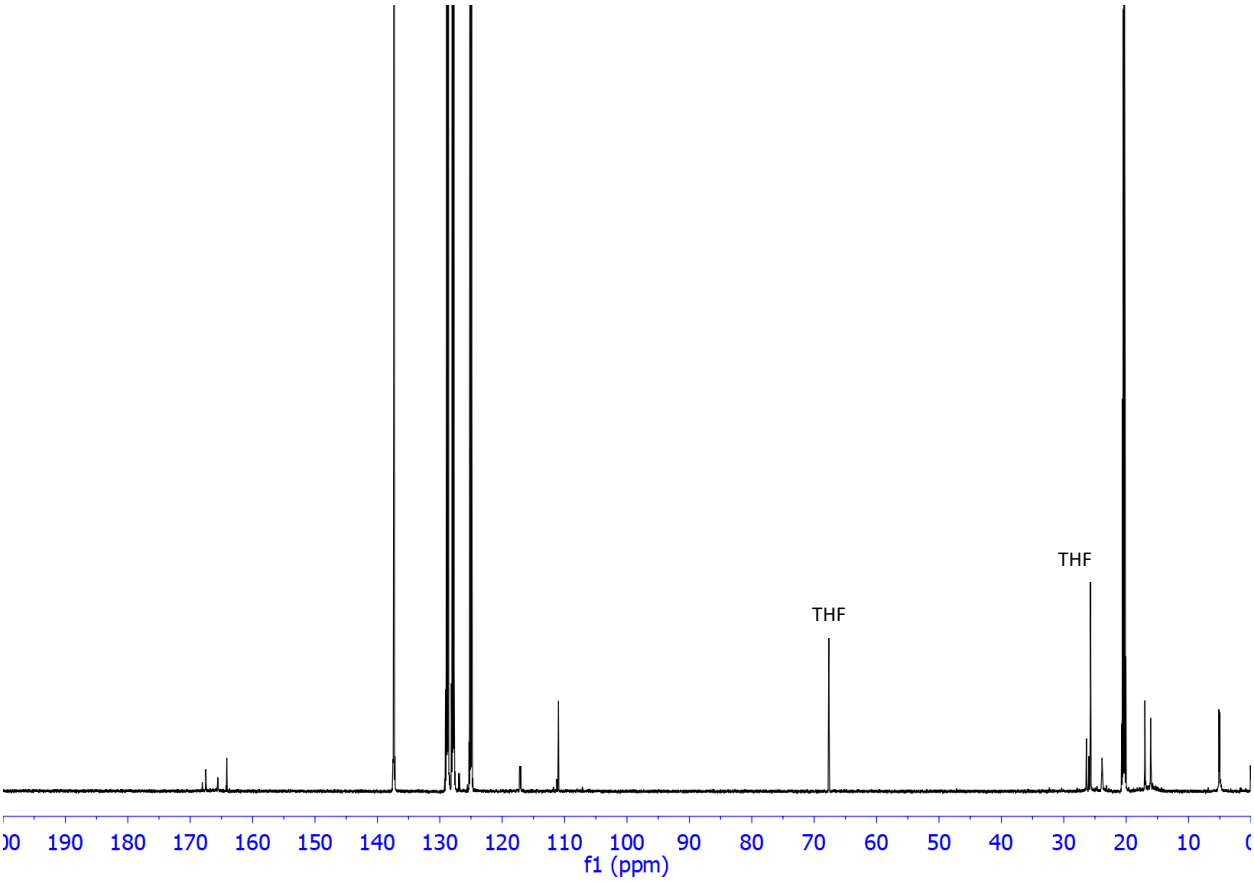

Figure S57. $^{13}C\{^{1}H\}$ NMR Spectrum of $L^{Pm}Lu(CH_2SiMe_3)_2$ in toluene-d_8 at ambient temperature.

$L^{Pm}LuCl_2$ (**13**):

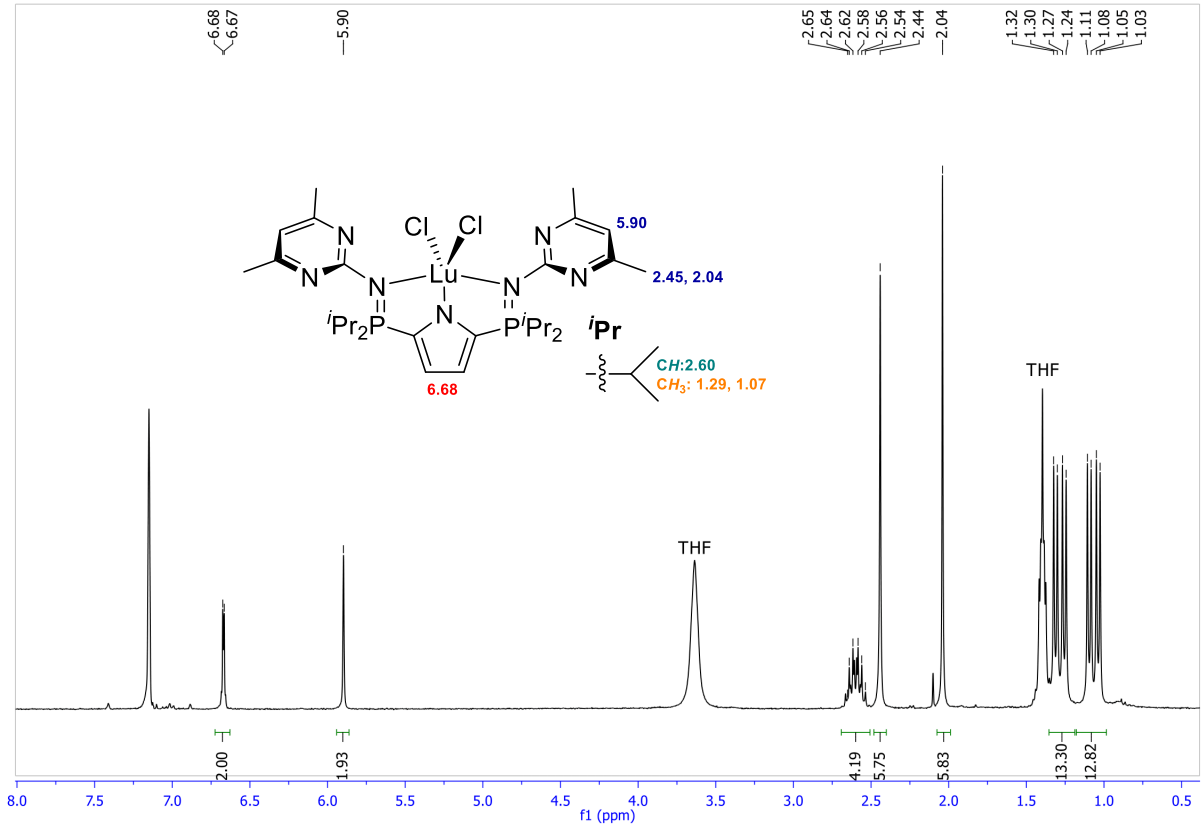

Figure S58. ^{1}H NMR Spectrum of $L^{Pm}LuCl_2$ in benzene-d_6 at ambient temperature.

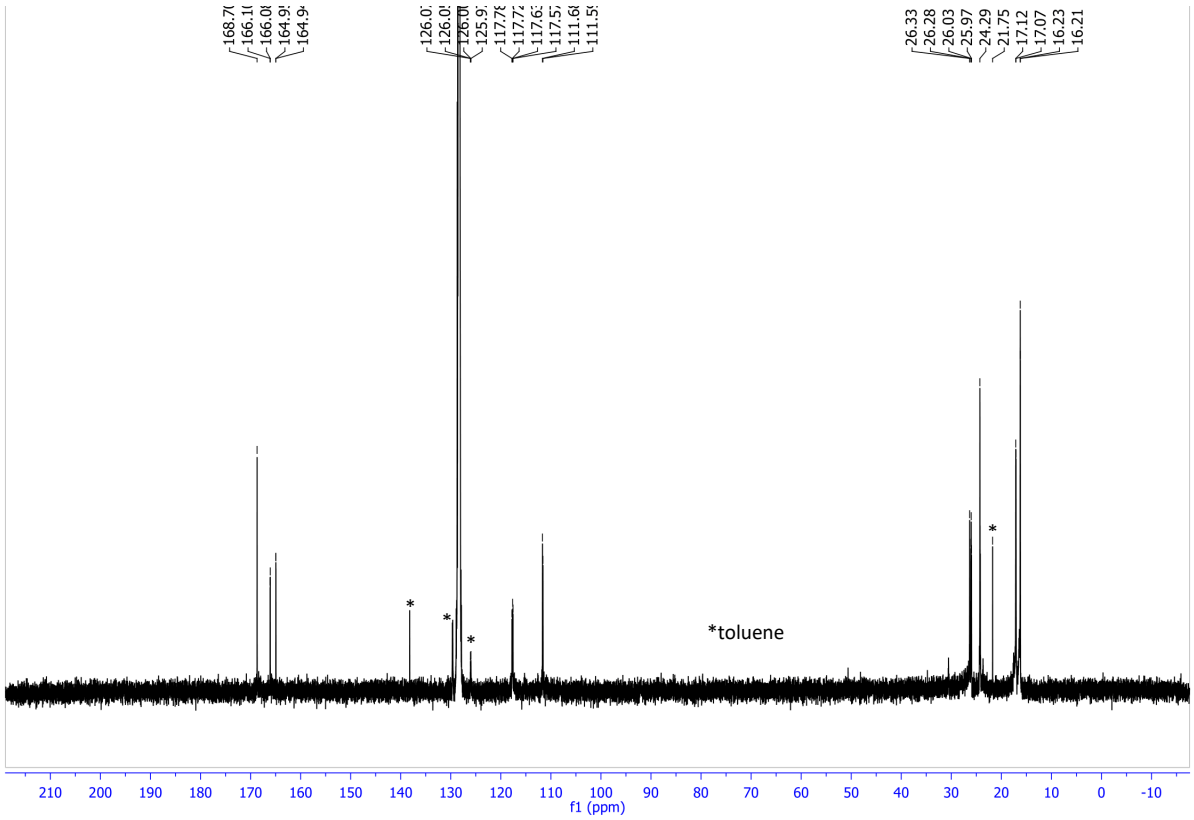

Figure S59. $^{13}C\{^{1}H\}$ NMR Spectrum of $L^{Pm}LuCl_2$ in benzene-d_6 at ambient temperature.

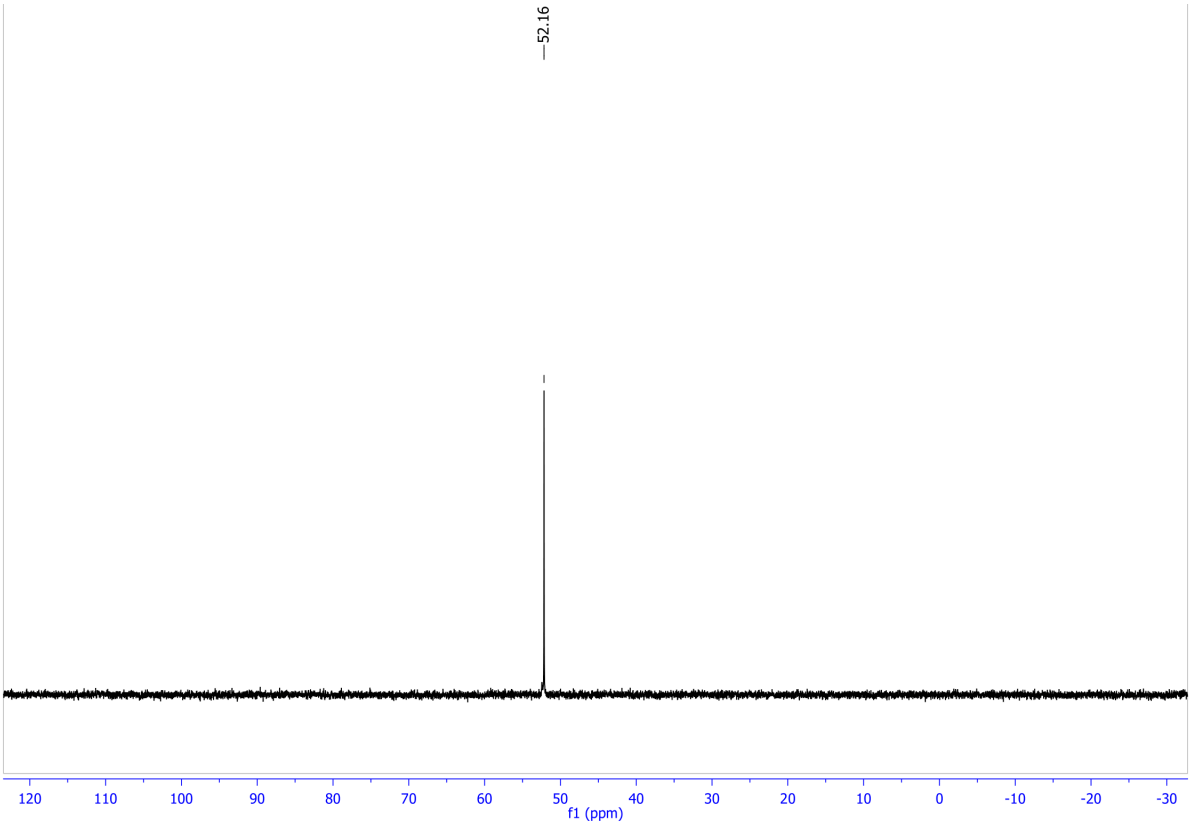

Figure S60. $^{31}P\{^{1}H\}$ NMR Spectrum of $L^{Pm}LuCl_2$ in benzene-d_6 at ambient temperature.

X-ray Crystallographic Refinement Tables for Complexes **5**, **6**, **7$_{CPh3}$**, **7$_{Dipp}$**, **8$_{CPh3}$**, **8$_{Dipp}$**, **11,** and **13**

Table 1. X-ray Crystallographic Refinement Tables for Complexes **5**, **6** and **7$_{CPh3}$**

	5	**6**	**7$_{CPh3}$**[a]
Formula	$C_{44}H_{70}N_3P_2ScSi_2$	$C_{42}H_{74}LuN_3P_2Si_2$	$C_{122}H_{149}Lu_2N_8P_4Si_2$
FW/g•mol^{-1}	804.11	914.13	2263.49
Crystal System	Monoclinic	Monoclinic	Triclinic
Space Group	$P2_1/n$	$P2_1/n$	P–1
a (Å)	16.3033(2)	11.2152(3)	12.31417(13)
b (Å)	17.2331(2)	17.6224(5)	21.4332(2)
c (Å)	17.6226(2)	24.0711(6)	24.4686(2)
α (°)	90	90	110.2276(10)
β (°)	105.8330(10)	92.481(2)	104.4073(10)
γ (°)	90	90	92.0411(9)
Volume (Å^3)	4763.34(10)	4752.9(2)	5816.40(11)
Z	4	4	2
D_{calc} (g•cm^{-3})	1.121	1.277	1.292
μ (mm^{-1})	2.664	2.224	4.262
Crystal Size (mm)	0.05 × 0.03 × 0.01	0.08 × 0.05 × 0.01	0.05 × 0.05 × 0.03
θ range (°)	7.314 to 155.262	6.71 to 61.124	6.984 to 160.818
K_α (nm)	1.54184	0.71073	1.54184
N	47565	54775	131024
N_{ind}	9885	11880	25332
Data/restraints/parameters	9883/2/512	11880/0/469	25332/0/1209
GoF on F^2	1.055	1.036	1.058
R_1 (I>2σ(I))[b]	0.0414	0.0369	0.0582
wR_2 (I>2σ(I))[c]	0.1110	0.0888	0.1627
$\Delta\rho_{max}$ and $\Delta\rho_{min}$ (e•Å^3)	0.43/–0.73	2.35/–0.75	2.39/–3.25

Notes: [a]Crystallized with one molecule of disordered heptane in the asymmetric unit. [b]$R_1 = \Sigma||F_o|-|F_c||/\Sigma|F_c|$. [c]$wR_2 = \{\Sigma[w(F_o^2-F_c^2)^2]/\Sigma[w(F_o^2)^2]\}^{1/2}$.

Table 2. Full Crystallographic Refinement Tables for Complexes $\mathbf{7_{Dipp}}$ and $\mathbf{8_{CPh_3}}$

	$\mathbf{7_{Dipp}}$	$\mathbf{8_{CPh_3}}$
Formula	$C_{50}H_{81}LuN_4P_2Si$	$C_{78}H_{96}LuN_5P_2$
FW/g•mol^{-1}	1003.18	1340.5
Crystal System	Monoclinic	Triclinic
Space Group	$P2_1$	P–1
a (Å)	11.59705(9)	12.74240(10)
b (Å)	20.55239(15)	14.66260(10)
c (Å)	11.79321(10)	20.5619(2)
α (°)	90	74.4510(10)
β (°)	113.2891(9)	89.2780(10)
γ (°)	90	71.2670(10)
Volume (Å^3)	2581.85(4)	3493.66(6)
Z	2	2
D_{calc} (g•cm^{-3})	1.290	1.274
μ (mm^{-1})	4.723	3.475
Crystal Size (mm)	0.3 × 0.2 × 0.1	0.1 × 0.05 × 0.03
ϑ range (°)	8.162 to 160.298	6.628 to 160.86
K_α (nm)	1.54184	1.51184
N	30369	79766
N_{ind}	10423	15242
Data/restraints/parameters	10423/1/553	15242/0/740
GoF on F^2	1.089	1.114
R_1 (I>2σ(I))[a]	0.0298	0.0311
wR2 (I>2σ(I))[b]	0.0760	0.0865
$\Delta\rho_{max}$ and $\Delta\rho_{min}$ (e•Å^3)	0.63/–0.70	1.38/–1.14

Notes: [a] $R_1 = \Sigma||F_o|-|F_c||/\Sigma|F_c|$. [b] $wR_2 = \{\Sigma[w(F_o^2-F_c^2)^2]/\Sigma[w(F_o^2)^2]\}^{1/2}$.

Table 3. X-ray Crystallographic Refinement Tables for Complexes **8_{Dipp}**, **11,** and **13**

	8_{Dipp}	**11**	**13**
Formula	$C_{58}H_{88}LuN_5P_2$	$C_{28}H_{45}N_7P_2$	$C_{35}H_{52}Cl_2LuN_7P_2$
FW/g•mol^{-1}	1092.24	541.65	878.64
Crystal System	Monoclinic	Monoclinic	Monoclinic
Space Group	$P2_1/n$	$P2_1/n$	I2/a
a (Å)	14.96740(10)	11.09120(10)	19.5525(5)
b (Å)	17.02750(10)	24.3906(2)	13.3420(3)
c (Å)	21.66410(10)	11.85320(10)	30.8950(7)
α (°)	90	90	90
β (°)	95.2220(10)	108.5340(10)	99.413(2)
γ (°)	90	90	90
Volume (Å^3)	5498.34(6)	3040.23(5)	7951.0(3)
Z	4	4	8
D_{calc} (g•cm^{-3})	1.319	1.183	1.468
μ (mm^{-1})	4.285	1.515	2.732
Crystal Size (mm)	0.3 × 0.3 × 0.1	1.0 × 0.8 × 0.5	0.7 × 0.5 × 0.5
ϑ range (°)	6.615 to 160.668	7.248 to 159.99	6.788 to 61.502
K_α (nm)	1.54184	1.51184	0.71073
N	64880	33645	48568
N_{ind}	11972	6555	10026
Data/restraints/parameters	11972/0/621	6555/0/346	10026/0/437
GoF on F^2	1.099	1.075	1.023
R_1 (I>2σ(I))[a]	0.0297	0.0398	0.0223
wR2 (I>2σ(I))[b]	0.0754	0.1035	0.0508
$\Delta\rho_{max}$ and $\Delta\rho_{min}$ (e•Å^3)	0.67/–0.90	0.32/–0.39	0.92/–0.56

Notes: [a] $R_1 = \Sigma||F_o|-|F_c||/\Sigma|F_c|$. [b] $wR_2 = \{\Sigma[w(F_o^2-F_c^2)^2]/\Sigma[w(F_o^2)^2]\}^{1/2}$.